

Modeling of muscle tissue: a multiphase model using continuum mechanics

Politecnico di Milano



POLITECNICO
MILANO 1863

M.Sc. Thesis of
Lorenzo Caranti
Matr. 897938

Supervisor : Pasquale Ciarletta
Co-Supervisor: Alfredo Marzocchi

Programme: *Mathematical Engineering*

Department of Mathematics

Anno accademico: 2019/2020

July 8, 2020

Abstract

Mathematical modeling of muscle tissue, in particular of its contraction, has become an important topic in biomechanics and biomedical fields. There exist some models, based on continuum mechanics, which describe the activation of a muscle, either by using a multiplicative decomposition of the deformation gradient, like *active strain*, or an additive split of the energy, called *active stress*. Moreover there exists a model called *mixture active strain* approach, which takes advantage of the multiplicative decomposition only on the anisotropic component of the energy, that permits to model muscle activation with a constant parameter, while recovering the uniaxial deformation experimental data more accurately. Considering the muscle as a *fiber-reinforced material*, we show why the choice of an energy dependent on both anisotropic invariants is more compatible with experimental data which investigate the shear responses of an anisotropic body. Lastly we introduce a new model, using *mixture active strain* approach, which better reproduces the experimental data of the stress-stretch curve.

Sintesi

La contrazione muscolare è un argomento molto discusso in ambito biomedico, in particolare per quel che riguarda l'attivazione del muscolo. Una categoria di materiali in cui rientrano i muscoli è infatti quella dei materiali attivi, capaci di deformarsi senza carichi esterni. Attraverso la meccanica dei continui sono stati sviluppati diversi modelli in grado di descrivere il comportamento di questo tipo di materiali, come l'*active strain* che sfrutta una decomposizione moltiplicativa del tensore gradiente di deformazione, o l'*active stress*, che divide l'energia in una somma di energia attiva ed energia passiva. Un altro modello utilizzato è il *mixture active strain*, che utilizza la decomposizione moltiplicativa soltanto sulla componente anisotropa dell'energia, permettendo di ottenere una migliore previsione dei dati di deformazione uniassiale, mantenendo il parametro di attivazione costante. Una scelta che viene spesso effettuata è quella di far dipendere la parte anisotropa dell'energia solo dal quarto invariante, ma questo porta a risultati controintuitivi fisicamente e in disaccordo con i risultati sperimentali. Infine introduciamo un modello dipendente da entrambi gli invarianti, che grazie al modello *mixture active strain* riesce a prevedere in maniera migliore i dati di deformazione uniassiale.

Contents

Abstract	ii
Sintesi	iii
Contents	iv
Summary	v
List of figures	vi
List of tables	vii
1 Introduction to skeletal muscles: biological structure and experimental data	1
1.1 Muscle structure and activation	1
1.2 Hawkins and Bey's data	3
2 Mathematics of Continuum Mechanics and Nonlinear Elasticity	6
2.1 Preliminary notions of Continuum Mechanics and Hyperelasticity	6
2.1.1 Kinematics, constitutive laws and conservation laws	7
2.1.2 Notions of Elasticity and Hyperelasticity	10
2.2 State of art of passive behaviour of muscle tissue	15
3 Active Stress vs Active Strain approaches	19
3.1 The active stress approach	19
3.2 The active strain approach	22
4 A novel multiphase model with active strain	28
4.1 The mixture active strain approach	28
4.2 Anisotropy and representation by invariants	33
4.3 Results of proposed models: prediction on experimental data	36
Conclusions	46
Acknowledgements	47
Bibliography	47

Summary

In order to provide a mathematical description of muscles, like skeletal muscles or the cardiac muscle, an open research topic in the field of biomechanics has become the modeling of soft biological tissues and numerical methods for simulations. In particular, a topic of interest is the one regarding what are the so called *active materials*, materials that can undergo deformation even without any external load, like muscles, which under an electrical stimulus have actin and myosin heads attaching in order to shorten the muscle in a preferred direction, to provide force and movement. In order to describe this behaviour we use the framework of Continuum Mechanics, where it's studied how a body deforms under, for example, external loads. Here we assume that the body is an anisotropic material, which means that it has a preferential direction, given by the orientation of the fibers, and an incompressible material, thanks to the fact that it is mainly made of water. In particular, we will set in the framework of Hyperelasticity, and consider the muscle tissue as a *fiber-reinforced material*, which is described as an anisotropic material embedded in an isotropic material, to reproduce the behaviour of the muscle fibers and the collagen material surrounding them.

A model which is particularly suitable for this type of materials is the so called *mixture active strain approach*, which enables to activate only a part of the body (in our case the anisotropic one).

In Chapter 1 we show the main functions of the muscle tissue and in particular the structure of skeletal muscle tissue, then we illustrate the data obtained by Hawkins and Bey [4] in their experiments in vivo on a *tibialis anterior* of rats, to obtained realistic data in order to test our new model.

In Chapter 2 we recall the bases of Continuum Mechanics and Hyperelasticity, then we show two classical models to describe the passive behaviour of the muscle tissue. In Chapter 3 we recall two classical models which describe the behaviour of activated muscle tissue: the *active stress* which uses an additive decomposition of the strain energy function, and the *active strain* which takes advantage of a multiplicative decomposition of the deformation gradient.

In Chapter 4 the work is divided as follows. First we introduce the *mixture active strain* method, which uses the multiplicative decomposition of the active strain approach only in the anisotropic part of the material, giving the possibility of a better fit of the data by Hawkins and Bey using a constant activation.

Second, we introduce the work by Murphy[3], which shows how the dependence of the strain energy on only one of the anisotropic invariants implies physical controtuitive conditions on the shear moduli, that moreover are shown to be wrong by experimental data.

Lastly we introduce a new model depending on both invariants, and test it on Hawkins and Bey experimental data.

List of Figures

1.1	Muscle macroscopic structure	2
1.2	Muscle microscopic structure	2
1.3	Parallel and pennate muscles	3
1.4	Hawkins and Bey's data plot	4
2.1	Displacement representation	7
2.2	Exponential model's fit on Hawkins and Bey's data	16
2.3	Gent model's fit on Hawkins and Bey's data	17
3.1	Active stress along fibers and Hawkins and Bey's active data	21
3.2	Gent's model fit on Hawkins and Bey's data	21
3.3	Kröner-Lee decomposition	22
3.4	Passive stress along fibers and Hawkins and Bey's active data	23
3.5	Activation behaviour with respect to λ , with γ constant, $\gamma = 0.05, 0.1, 0.15$	24
3.6	Activation behaviour with respect to λ	25
3.7	Total stress-strain relation and Hawkins and Bey's data	26
4.1	Plot of P_M when $\mu = 1.8kPa$, $I_{max} = 0.41$, $\alpha = 31kPa$, $\beta = 1.5$ and γ varies from 0 to 0.5 with steps of 0.05.	31
4.2	Plot of the anisotropic component where γ varies from 0 to 0.5 with steps of 0.05.	32
4.3	Active contribution of the model and active experimental data.	32
4.4	Stress-strain relation with energy by Horgan and Saccomandi when $\mu = 1.5$ kPa, $I_{max} = 0.41$, $c_1 = -63.51$ kPa, $c_2 = -10.54$ kPa, $c_3 = 0.62$ kPa, $c_4 = -0.068$ kPa, $c_5 = -0.867$ kPa, $c_6 = -847$ kPa and $\gamma = 0.494$	38
4.5	Stress-strain relation with active component of the energy by Horgan and Saccomandi when $\mu = 1.5$ kPa, $I_{max} = 0.41$, $c_1 = -63.51$ kPa, $c_2 = -10.54$ kPa, $c_3 = 0.62$ kPa, $c_4 = -0.068$ kPa, $c_5 = -0.867$ kPa, $c_6 = -847$ kPa and $\gamma = 0.494$	39
4.6	Stress-strain relation with energy by Masson et al. when $\mu = 2$ kPa, $I_{max} = 0.41$, $c_1 = -3.501$ kPa, $c_2 = -22.5908$ kPa, $c_3 = 0.044$ kPa, $c_4 = -0.624$ kPa and $\gamma = 0.481$	40
4.7	Active component of the stress-strain relation with energy by Masson et al. when $\mu = 2$ kPa, $I_{max} = 0.41$, $c_1 = -3.501$ kPa, $c_2 = -22.5908$ kPa, $c_3 = 0.044$ kPa, $c_4 = -0.624$ kPa and $\gamma = 0.481$	41
4.8	Plot of P_M when $\mu = 2.3$ kPa, $I_{max} = 0.41$, $c_1 = 6.21$ kPa, $c_2 =$ 15.5462 kPa, $c_3 = -0.3697$ kPa, $c_4 = 0.0116$ kPa and $\gamma = 0.5556$	42
4.9	Plot of the active part P_M	43

List of Tables

4.1 Contributions of single anisotropic activated terms.	44
--	----

Chapter 1

Introduction to skeletal muscles: biological structure and experimental data

In this chapter we will introduce how muscles are made and how they activate, then we will look at the data by Hawkins and Bey in [4] and see what we can understand from them.

1.1 Muscle structure and activation

Muscle tissue is used by the body for some fundamental functions which can be really different from each other. These functions can be the movement of the body parts, moving the blood in the vessels, moving organs to assist digestion or many others. The high variability of the tasks of this tissue requires it to be differentiated in more types. In fact there exist three types of muscles :

- the *skeletal muscle*, which moves the body and its parts
- the *cardiac muscle*, that determines, with his contraction, the blood flow
- the *smooth muscle*, responsible for organs movement and which assists some physiological functions

Each one of these muscles is made by specific cells, which are all contractile units, that under electrical and chemical stimulus can shorten and develop force. The type of tissue we'll be interested in is the *skeletal muscle tissue*, which makes up to 40-45% of body mass and it's in about 660 muscles of the human body. Its morphological units are called *fibers*, that are cells with an elongated form with a diameter variable from 10 to 100 μm and whose number in various skeletal muscles can be highly different.

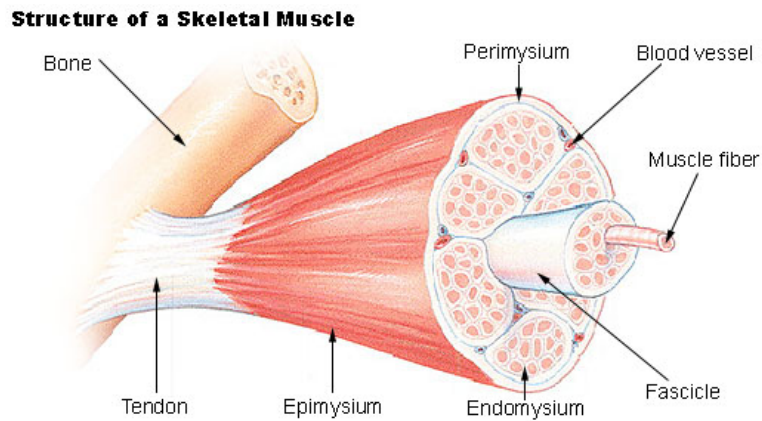


Figure 1.1: Muscle macroscopic structure

As shown in Figure 1.1 every muscular fiber is surrounded by connective tissue which separates adjacent cells, called *endomysium*, then groups of around 150 fibers are called fascicles and are surrounded by another winding of connective tissue called *perimysium*. Finally, the whole muscle is sheathed in a last layer of connective tissue, called *epimysium*, which becomes thicker at the end, anchoring the muscle to the tendons at each end. Tendons are structures made of collagen which transfer the tension produced by the fibers to the bones.

While the connective tissue can be considered isotropic, the fibers are transversely isotropic, since they can be considered cylindrical and contract along their axis.

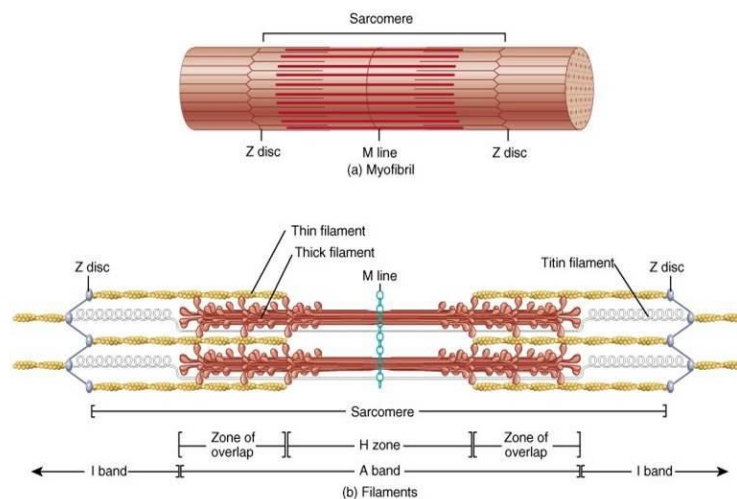


Figure 1.2: Muscle microscopic structure

In Figure 1.2 we see that on a microscopic level, fibers are made of *myofibrils*, which have a diameter of about $1\text{-}2\ \mu\text{m}$ and are made by units which repeat regularly along them. These units, called *sarcomeres*, with a resting length of about $2,5\ \mu\text{m}$, are responsible for the contraction of the fibers. Every sarcomere is made by thin ($1\ \mu\text{m}$ long and with a diameter of about $5\ \text{nm}$) and thick ($1,6\ \mu\text{m}$ long and with a diameter of $15\ \text{nm}$) filaments. Thin filaments are made of actin and are anchored

to the end region of the sarcomere which is called *Z-disc*, while thick filaments are made of myosin, and are disposed in the central region of the sarcomere, where their disposition gives rise to darker bands, called *A-bands*. Then moreover, two more zones can be observed : the *I-band* which is the zone where there are only actin filaments, and the *H-zone* which is a lighter band where there are only thick myosin filaments.

The sarcomere represents the contractile unit of the muscle, since when exposed to electrical stimulus by the nervous system, the *Z-discs* get closer thanks to the fact that thin and thick filaments slide on each other. In particular, when the sarcomere activates, the myosin heads grab on to the actin filaments and rotate, generating what is called a *cross-bridge*. Influencing the contraction effect of the muscle there are several factors, like the amount of connective tissue, the length of the fibers, which can shorten up to 60% of their rest length, and the muscular architecture. The muscular architecture substantially refers to the orientation of the fibers with respect to the direction which the force is generated macroscopically. This splits up the fibers and consequently the muscles in two types, when the fibers are parallel to the direction of the force-generating axis the muscles are called parallel, when they have a different orientation the muscle is called pennate.

In Figure 1.3 we can see the principal types of muscle direction.

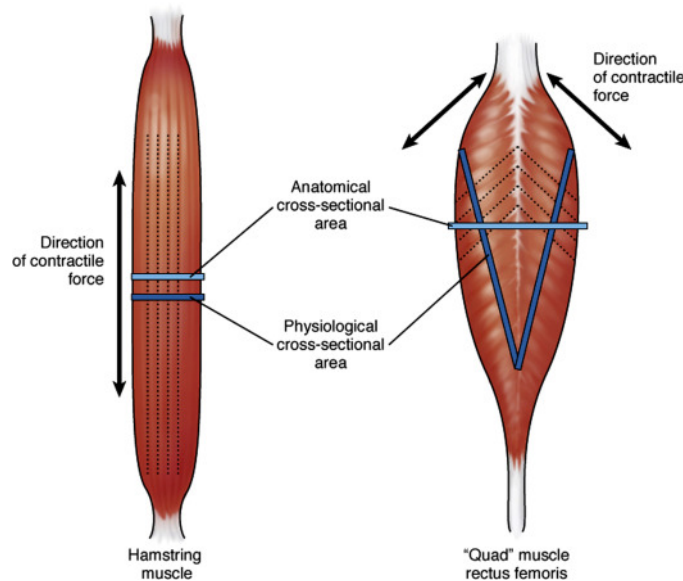


Figure 1.3: Parallel and pennate muscles

1.2 Hawkins and Bey's data

The data collected by Hawkins and Bey in [4] are useful to compare our models with the results from experiments. These data show the behaviour of the stress-stretch relationship of a muscle on relaxed state and on activated state. The experiment has been conducted in vivo on a rat's tetanized *tibialis anterior*, considering the fact that the tension produced is divided into a passive and an active contribution. First the passive data were collected, then by electrical stimulus the muscle was activated and the total data (passive and active contribution) were collected. The stretch in

the data has been divided by the resting length of the muscle, so that λ shows the ratio of elongation, in fact $\lambda = 1$ means that the muscle is at its resting length and it's unstressed.

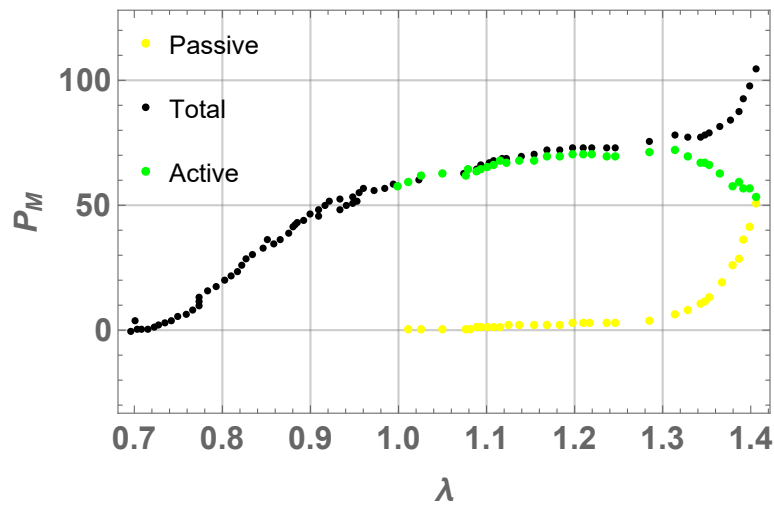


Figure 1.4: Hawkins and Bey's data plot

Now first we focus on the passive curve, shown in Figure 1.4. The first thing that can be noticed is the exponential behaviour after a certain stretch ($\lambda \approx 1.3$) given by the connective tissue, which rebounds, but before that length there is only a very small resistance. When the muscle is activated the fibers shorten, so that the new unstressed length will be much less than the passive resting length; in fact we see it on the total curve, which starts showing stress already around $\lambda = 0.7$. Subtracting the passive curve from the total curve we get the active curve, that is the contribution given by only the active part of the tissue. This curve shows us that the active contribution has a peak around $\lambda = 1.3$, that is when all the cross-bridges in the sarcomere are formed. This explains the behaviour of the total curve after $\lambda = 1.3$, in fact we can see the same exponential behaviour as in the passive curve, that is because the activation is complete and the elastic behaviour of the connective tissue prevails.

Chapter 2

Mathematics of Continuum Mechanics and Nonlinear Elasticity

In this chapter we are going to recall the basic notions of the theory of Continuum Mechanics and Hyperelasticity required to model soft biological tissues. First we will introduce some balance equations, then we introduce a framework that will lead to more complicate and accurate models. The tissue we will model is the skeletal muscle tissue, which can be considered as an anisotropic (more specifically transversely isotropic) continuum material, since it has a preferential direction, and incompressible, since it's composed up to 75% of water.

Later on we will consider the material to be hyperelastic, neglecting viscous effects and considering a steady state, we will introduce some classical models proposed to describe the passive state of the muscle tissue, and which are coherent with Hawkins and Bey's experimental data.

2.1 Preliminary notions of Continuum Mechanics and Hyperelasticity

In continuum mechanics a body is considered as a 3D continuous domain \mathcal{B}_0 , whose varying shape in time becomes \mathcal{B}_t . The motion of a body can be described by the *displacement* $\chi : \mathcal{B}_0 \subset \mathbb{R}^3 \rightarrow \mathbb{R}^3$, which is an invertible smooth map describing how every point is mapped from \mathcal{B}_0 to \mathcal{B}_t .

Every point \mathbf{X} in \mathcal{B}_0 , which is called reference configuration, is associated with $\mathbf{x} = \chi(\mathbf{X}, t)$, its current placement in the so called current configuration \mathcal{B}_t .

\mathbf{X} are called *material coordinates*, and represent the position of a particle in the reference configuration \mathcal{B}_0 , while \mathbf{x} are called *spatial coordinates* and show the position of a particle in the current configuration.

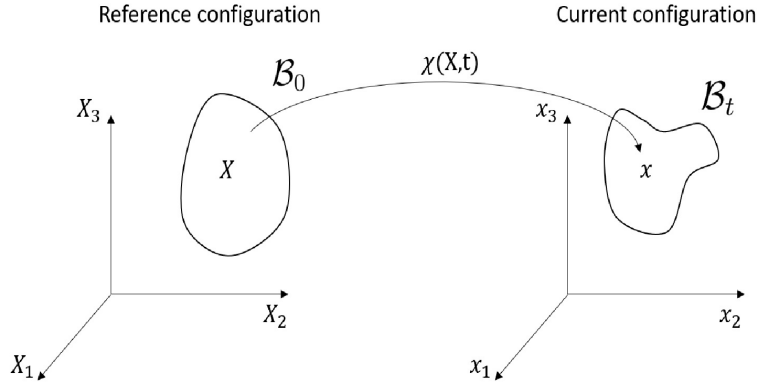


Figure 2.1: Displacement representation

2.1.1 Kinematics, constitutive laws and conservation laws

Let us introduce first the *deformation gradient* tensor \mathbf{F} defined as

$$\mathbf{F} := \frac{\partial \mathbf{x}}{\partial \mathbf{X}} = \text{grad}(\mathbf{x})$$

and its determinant $J := \det \mathbf{F}$. We assume that $J > 0$ since it represents the ratio between initial and actual volume.

Now let us introduce the *material velocity* $\mathbf{V} : \mathcal{B} \times \mathbb{R} \rightarrow \mathbb{R}^3$ which is defined as

$$\mathbf{V}(\mathbf{X}, t) := \frac{\partial \chi}{\partial t}(\mathbf{X}, t)$$

which represents the velocity at time t of the particles which were in \mathbf{X} in the reference configuration, and the *Eulerian velocity*,

$$\mathbf{v}(\mathbf{x}, t) := \mathbf{V}(\chi^{-1}(\mathbf{x}; t), t)$$

which depends on spatial coordinates and gives the velocity of the particles which are in \mathbf{x} at time t .

Now we will introduce an important theorem of Continuum mechanics.

Theorem 2.1.1 (Reynolds' Transport Theorem). *Let $\Omega(t)$ be a regular region in \mathcal{B}_t and $v_n(x, t)$ be the outward normal speed of a surface point $\mathbf{x} \in \partial\Omega(t)$. Then for any smooth tensor field $F(\mathbf{x}, t)$, we have*

$$\frac{d}{dt} \int_{\Omega(t)} F(\mathbf{x}, t) dV = \int_{\Omega(t)} \frac{\partial F}{\partial t}(\mathbf{x}, t) dV + \int_{\partial\Omega(t)} F(\mathbf{x}, t) v_n(\mathbf{x}, t) dS$$

Next we suppose that there exists a function $\rho(\mathbf{x}; t)$ integrable and of class C^1 , which represents the *mass density* per unit volume of the current configuration. Then

$$M(\Omega(t)) = \int_{\Omega(t)} \rho(\mathbf{x}, t) dV$$

will represent the mass of a portion $\Omega(t)$ of the body in its current configuration. The *balance of mass* states that $\forall \Omega \subset \mathcal{B}_0$,

$$M(\Omega(t)) = M(\Omega)$$

which means that any subbody Ω doesn't vary his mass during the motion, and applying the Reynolds' Transport Theorem, using $F(\mathbf{x}, t) = \rho(\mathbf{x}, t)$ we can find that

$$\frac{d\rho}{dt} + \rho \operatorname{div} \mathbf{v} = 0$$

which is called *equation of continuity*.

Computing this equation, using a change of variables $\mathbf{x} = \chi(\mathbf{X}, t)$ we find that

$$J(\mathbf{X}, t) \rho(\chi(\mathbf{X}, t), t) = \rho_0(\mathbf{X})$$

where $J = \det \mathbf{F}$ and $\rho_0(\mathbf{X})$ represents the mass density in the reference configuration. If the material is incompressible we have that

$$\rho(\mathbf{X}, t) = \rho_0(\mathbf{X}, 0)$$

which gives

$$\det \mathbf{F} = 1.$$

Next we want to find out how forces interact with our subbody Ω at any time and forces and be divided into internal and external forces.

First, the resultant of the external forces can be represented as

$$\int_{\Omega(t)} \rho \mathbf{b} dV$$

where we've introduced $\mathbf{b}(\mathbf{x}, t)$, which is the *density of external forces* and it's usually known.

For what concerns the internal forces we will assume the following postulate.

Cauchy postulate. *If $\mathbf{x} \in \partial\Omega_{t_1} \cup \partial\Omega_{t_2}$, and $\partial\Omega_{t_1}$ and $\partial\Omega_{t_2}$ have a common oriented normal at x , then*

$$\mathbf{t}(\mathbf{x}, t, \partial\Omega_{t_1}) = \mathbf{t}(\mathbf{x}, t, \partial\Omega_{t_2})$$

which has as an immediate consequence the following theorem

Theorem 2.1.2 (Cauchy's lemma). *Suppose that $\mathbf{t}(\cdot, \mathbf{n})$ is a continuous function of \mathbf{x} . Then*

$$\mathbf{t}(\mathbf{x}, -\mathbf{n}) = -\mathbf{t}(\mathbf{x}, \mathbf{n})$$

for any $\mathbf{x} \in \Omega_t$ and any unit vector $\mathbf{n} \in \partial\Omega_t$.

Finally we have the last theorem, which states

Theorem 2.1.3 (Cauchy's Theorem). *Under the same conditions assumed in Cauchy's lemma, there exists a second-order tensor field \mathbf{T} , such that*

$$\mathbf{t}(\mathbf{x}, t, \mathbf{n}) = \mathbf{T}(\mathbf{x}, t)\mathbf{n}$$

These theorems basically state that internal forces interact with each other, resulting at the end only as surface forces.

We will assume that $\mathbf{T} = \mathbf{T}(\mathbf{F})$.

This tensor describes the tensional state in the current configuration, but since this configuration is not known a priori, it's useful to introduce its equivalent in the reference configuration, the *first Piola-Kirchhoff stress tensor*, given by

$$\mathbf{P} = J\mathbf{T}\mathbf{F}^{-T}$$

then we also introduce the *second Piola-Kirchhoff stress tensor* which is

$$\mathbf{S} = J\mathbf{F}^{-1}\mathbf{T}\mathbf{F}^{-T} = \mathbf{F}^{-1}\mathbf{P}$$

The first tensor is generally not symmetric, but satisfies the relation $\mathbf{P}\mathbf{T}^T = \mathbf{F}\mathbf{P}^T$, while the second is always symmetric.

Now we will introduce the *principle of conservation of linear momentum* which says that the rate of change of linear momentum of a material volume equals the resultant force on the volume:

$$\frac{d}{dt} \int_{\Omega(t)} \rho \mathbf{V} dV = \int_{\Omega(t)} \rho \mathbf{b} dV + \int_{\partial\Omega(t)} \mathbf{t} dS$$

from this, using the divergence theorem and some previous results, the Eulerian form of the *equation of motion* can be obtained

$$\rho \frac{d\mathbf{v}}{dt} = \rho \mathbf{b} + \text{div}(\mathbf{T})$$

which expressed in the reference configuration becomes

$$\rho_0 \frac{\partial^2 \mathbf{u}}{\partial t^2} = \rho_0 \mathbf{B} + \text{Div}(\mathbf{P})$$

where $\mathbf{u} = \mathbf{x} - \mathbf{X}$ is the *displacement*.

Finally we introduce the *conservation of angular momentum*, which reads

$$\frac{d}{dt} \int_{\Omega(t)} \rho \mathbf{x} \times \mathbf{v} dV = \int_{\Omega(t)} \rho \mathbf{x} \times \mathbf{b} + \int_{\partial\Omega(t)} \mathbf{x} \times \mathbf{t} dS$$

and which is satisfied if and only if $\mathbf{T} = \mathbf{T}^T$, giving some restriction on the Cauchy tensor \mathbf{T} . This restriction can also be seen on \mathbf{P} , since $\mathbf{P} = J\mathbf{T}\mathbf{F}^{-T}$ we have that the balances of linear and angular momentum are satisfied if and only if $\mathbf{P}\mathbf{F}^T = \mathbf{F}\mathbf{P}^T$. From now on we will be interested to the equilibrium configuration, so the problem we will be considering is

$$\begin{cases} \rho_0 \mathbf{B} + \text{Div } \mathbf{P} = 0 \\ \det \mathbf{F} = 1 \\ \mathbf{P}\mathbf{F}^T = \mathbf{F}\mathbf{P}^T \end{cases}$$

2.1.2 Notions of Elasticity and Hyperelasticity

To begin we will introduce two tensors, the *left* and *right Cauchy-Green stress tensor*, which are defined as

$$\begin{aligned} \mathbf{C} &= \mathbf{F}^T \mathbf{F} \\ \mathbf{B} &= \mathbf{F} \mathbf{F}^T \end{aligned}$$

and are both symmetric.

We recall the *polar decomposition theorem*, which says that since $J > 0$, the deformation gradient \mathbf{F} can be decomposed as follows:

$$\mathbf{F} = \mathbf{R}\mathbf{U} = \mathbf{V}\mathbf{R}$$

where \mathbf{U} and \mathbf{V} are symmetric positive definite tensors, and \mathbf{R} is a rotation. In particular we have that $\mathbf{U}^2 = \mathbf{C}$ and $\mathbf{V}^2 = \mathbf{B}$.

This decomposition permits us to see how the deformation \mathbf{F} is composed by a rotation and a stretch.

In particular, since the muscle is transversely isotropic, we want to define the *stretch* along a given direction \mathbf{m} , which is defined as follows

$$\lambda = |\mathbf{F}\mathbf{m}| = \sqrt{(\mathbf{C}\mathbf{m}) \cdot \mathbf{m}}$$

and represents the percentual increment of length.

A material is called *hyperelastic* when there exists a function Ψ such that

$$\begin{aligned} \Psi &: \mathcal{B}_0 \times M_+^{3 \times 3} \rightarrow \mathbb{R} \\ (\mathbf{X}, \mathbf{F}) &\rightarrow \Psi(\mathbf{X}, \mathbf{F}) \end{aligned}$$

called *elastic energy*, that is C^1 with respect to \mathbf{F} , and such that

$$\mathbf{P}_{ij} = \frac{\partial \Psi}{\partial \mathbf{F}_{ij}}$$

Now we want the elastic energy to be independent from the motion of the observer, so we assume what is called the *principle of frame indifference*:

$$\Psi(\mathbf{Q}\mathbf{F}) = \Psi(\mathbf{F}) \quad \forall \mathbf{Q} \in SO(3).$$

By assuming this principle, we can rewrite Ψ as a function of the tensor \mathbf{C}

$$\Psi(\mathbf{F}) = \tilde{\Psi}(\mathbf{C})$$

by taking $\mathbf{Q} = \mathbf{R}^T$ where \mathbf{R} is the rotation obtained by the polar decomposition theorem.

Furthermore this allows us to write the first Piola-Kirchhoff stress tensor as

$$\mathbf{P} = 2\mathbf{F} \frac{\partial \tilde{\Psi}}{\partial \mathbf{C}}$$

The next thing we want to consider is the fact that some materials are intrinsically symmetric, which means that there could be directions which will lead to the same result when the body is deformed.

For this reason we will introduce what is called a *material symmetry group* :

$$\mathbb{G} = \{\mathbf{Q} \in SO(3) : \mathbf{T}(\mathbf{F}\mathbf{Q}) = \mathbf{T}(\mathbf{F}) \forall \mathbf{F} \in Lin^+\}$$

where $SO(3)$ is the set of all rotations and Lin^+ is the set of positive determinant deformations.

In fact if the body is independent of the direction of deformation it is called *isotropic*, and we will have that $\mathbb{G} = SO(3)$, and consequently its elastic energy will have the following property:

$$\Psi(\mathbf{Q}\mathbf{C}\mathbf{Q}^T) = \Psi(\mathbf{C}) \quad \forall \mathbf{Q} \in SO(3)$$

Now it's useful to recall that for any tensor, in particular for \mathbf{C} , it's true that

$$\mathbf{C}^3 - I_1\mathbf{C}^2 + I_2\mathbf{C} - I_3\mathbf{I} = 0$$

where I_1 , I_2 , and I_3 are called *invariants* of \mathbf{C} and

$$\begin{aligned} I_1(\mathbf{C}) &= \text{tr } \mathbf{C} \\ I_2(\mathbf{C}) &= \frac{1}{2}[(\text{tr } \mathbf{C})^2 - \text{tr } \mathbf{C}^2] \\ I_3(\mathbf{C}) &= \det \mathbf{C} \end{aligned}$$

What we are interested in are the so called *transversely isotropic* materials, for which we introduce \mathbf{m} , the preferential direction of the material and the *structural tensor* $\mathbf{M} = \mathbf{m} \otimes \mathbf{m}$.

Their material symmetry group will be

$$\mathbb{G} = \{\mathbf{Q} \in SO(3) : \mathbf{Q}\mathbf{m} = \pm\mathbf{m}\}$$

and in particular for transversely isotropic materials there are two more invariants, I_4 and I_5 to be introduced.

$$\begin{aligned} I_4(\mathbf{C}, \mathbf{M}) &= \text{tr } \mathbf{C}\mathbf{M} \\ I_5(\mathbf{C}, \mathbf{M}) &= \text{tr } \mathbf{C}^2\mathbf{M} \end{aligned}$$

If a material is *isotropic* and we assume the *principle of frame indifference*, the elastic energy is only dependent on the first three invariants of \mathbf{C} , and we can write

$$\Psi = \widehat{\Psi}(I_1, I_2, I_3)$$

if a material is transversely isotropic, the energy will be dependent on the preferential direction, and more in particular on I_4 and I_5

$$\Psi = \widehat{\Psi}(I_1, I_2, I_3, I_4, I_5)$$

The muscle tissue is anisotropic, and in particular it can be seen as a *fiber-reinforced material* which is a class of transversely isotropic materials.

These materials are made by transversely isotropic material, like muscle fibers, enveloped in an isotropic material, in this case the connective tissue, and their elastic energy is structured as follows

$$\Psi = \Psi_{iso}(I_1, I_2, I_3) + \Psi_{ani}(I_4, I_5)$$

The first Piola-Kirchhoff tensor can now be expressed as

$$\mathbf{P} = \frac{\partial \Psi}{\partial \mathbf{F}} = \frac{\partial \Psi}{\partial I_i} \frac{\partial I_i}{\partial \mathbf{F}} \quad (2.1)$$

So now its useful to recall the invariant's derivatives with respect to \mathbf{F}

$$\begin{aligned} \frac{\partial I_1}{\partial \mathbf{F}} &= 2\mathbf{F} \\ \frac{\partial I_2}{\partial \mathbf{F}} &= 2(I_1\mathbf{F} - \mathbf{F}^T\mathbf{F}) \\ \frac{\partial I_3}{\partial \mathbf{F}} &= \det \mathbf{F}\mathbf{F}^{-T} \\ \frac{\partial I_4}{\partial \mathbf{F}} &= 2\mathbf{F}\mathbf{M} \\ \frac{\partial I_5}{\partial \mathbf{F}} &= 2\mathbf{F}(\mathbf{C}\mathbf{M} + \mathbf{M}\mathbf{C}) \end{aligned}$$

Furthermore since the muscle is made mainly of water, we will assume that it is an incompressible material, so we need to meet the condition

$$J = 1$$

where $J = \det \mathbf{F}$.

This condition will introduce forces that will maintain the volume constant so we will need to introduce new forces in the conservation of linear momentum equation. In particular these forces are introduced by a lagrangian multiplier p , which we will call *pressure* and which modifies the first Piola-Kirchhoff tensor as follows

$$\mathbf{P} = \frac{\partial \Psi}{\partial \mathbf{F}} - p\mathbf{F}^{-T}$$

Now we will introduce two basic deformations for an isotropic elastic body, uniaxial stretch and simple shear, which we will use in the following chapters.

The first deformation we are going to see is the uniaxial stretch

$$x = \lambda_1 X, \quad y = \lambda_2 Y, \quad z = \lambda_3 Z$$

so that the deformation gradient will be

$$\mathbf{F} = \begin{bmatrix} \lambda_1 & 0 & 0 \\ 0 & \lambda_2 & 0 \\ 0 & 0 & \lambda_3 \end{bmatrix}$$

in this case $\lambda_i > 0$ represents an extension of the body in the direction \mathbf{e}_i , and $\lambda_i < 0$ a compression.

In particular if we impose incompressibility the deformation gradient will be

$$\mathbf{F} = \begin{bmatrix} \lambda & 0 & 0 \\ 0 & \frac{1}{\sqrt{\lambda}} & 0 \\ 0 & 0 & \frac{1}{\sqrt{\lambda}} \end{bmatrix}$$

so that when the body extends in a direction, it will be compressed along the other directions in order to maintain the volume constant.

In this case the first three invariants will be

$$I_1 = \lambda^2 + 2\lambda^{-1}, \quad I_2 = 2\lambda + \lambda^{-2}, \quad I_3 = 1$$

The second deformation we are going to introduce is the simple shear:

$$x = X + \kappa Y, \quad y = Y, \quad z = Z$$

where κ is a constant that represents the amount of shear.

The deformation gradient will be

$$\mathbf{F} = \begin{bmatrix} 1 & \kappa & 0 \\ 0 & 1 & 0 \\ 0 & 0 & 1 \end{bmatrix}$$

and consequently the invariants will be

$$I_1 = 3 + \kappa^2, \quad I_2 = 3 + \kappa^2, \quad I_3 = 1$$

Lastly, we want the elastic energy to have some mathematical properties, to ensure that problems are well-posed. In fact in an hyperelasticity the following problem

$$\begin{cases} \rho_0 \mathbf{B} + \text{Div} \frac{\partial \Psi}{\partial \mathbf{F}} = 0 \\ \det \mathbf{F} = 1 \\ \mathbf{P} \mathbf{F}^T = \mathbf{F} \mathbf{P}^T \end{cases}$$

can be reduced to a minimization problem.

First of all we introduce the definition of a *convex* function:

Definition. A function $F : M^{3 \times 3} \rightarrow \mathbb{R} \cup \{+\infty\}$ is called *convex* if

$$\alpha F(\mathbf{H}) + (1 - \alpha)F(\mathbf{G}) \geq F(\alpha \mathbf{H} + (1 - \alpha)\mathbf{G})$$

for each $\mathbf{H}, \mathbf{G} \in M^{3 \times 3}$, $\alpha \in (0, 1)$

Next one is *rank-one convexity*:

Definition. A function $F : M^{3 \times 3} \rightarrow \mathbb{R} \cup \{+\infty\}$ is called *rank-one convex* if for any couple of matrices $\mathbf{A}, \mathbf{B} \in M^{3 \times 3}$ with $\text{rank}(\mathbf{A} - \mathbf{B}) \leq 1$ and for any $0 < \lambda < 1$ we have that

$$F(\lambda \mathbf{A} + (1 - \lambda) \mathbf{B}) \leq \lambda F(\mathbf{A}) + (1 - \lambda) F(\mathbf{B}).$$

Next we introduce a stronger mathematical property, which implies rank-one convexity, called *polyconvexity*

Definition. A function $\Psi : M^{3 \times 3} \rightarrow \mathbb{R} \cup \{+\infty\}$, such that

$$\Psi(\mathbf{F}) = g(\mathbf{F}, \text{Cof } \mathbf{F}, \det \mathbf{F})$$

with $g : \mathbb{R}^{19} \rightarrow \mathbb{R} \cup \{+\infty\}$ convex, is called *polyconvex*.

Convexity implies policonvexity and consequently rank-one convexity, as shown in the following theorem

Theorem 2.1.4. *Let $F : M^{3 \times 3} \rightarrow \mathbb{R} \cup \{+\infty\}$ be convex. Then F is also polyconvex and rank-one convex.*

Finally the following theorem, which states under which conditions our problem will be well-posed

Theorem 2.1.5 (John Ball).

Let $\Psi : M_+^{3 \times 3} \rightarrow \mathbb{R}$ be a stored energy function, such that

(i) Ψ is polyconvex

(ii) if $\mathbf{F}_n \rightarrow \mathbf{F}$ in $M_+^{3 \times 3}$, $\mathbf{H}_n \rightarrow \mathbf{H}$ in $M_+^{3 \times 3}$, and $\delta_n \rightarrow 0^+$, then

$$\lim_{n \rightarrow +\infty} g(\mathbf{F}_n, \mathbf{H}_n, \delta_n) = +\infty$$

where $g : \mathbb{R}^{19} \rightarrow \mathbb{R} \cup \{+\infty\}$ is the convex function of polyconvexity definition;

(iii) There exist $a \in \mathbb{R}$, $b > 0$, $p \geq 2$, $q \in \mathbb{R}$ with $\frac{1}{p} + \frac{1}{q} \leq 1$, and $r > 1$, such that

$$g(\mathbf{F}, \mathbf{H}, \delta) \geq a + b(\|\mathbf{F}\|^p + \|\mathbf{H}\|^q + \delta^r)$$

for all $(\mathbf{F}, \mathbf{H}, \delta) \in M^{3 \times 3} \times M^{3 \times 3} \times (0, +\infty)$.

Let $\Omega \subset \mathbb{R}^3$ be a bounded open subset with boundary $\Gamma = \Gamma_0 \cup \Gamma_1$, where $|\Gamma_0| > 0$.

Let $\mathbf{f} : \Omega \rightarrow \mathbb{R}^3$ and $\mathbf{t} : \Gamma_1 \rightarrow \mathbb{R}^3$ measurable, such that

$$L[\mathbf{u}] = \int_{\Omega} \mathbf{f} \cdot \mathbf{u} \, dV + \int_{\Gamma_1} \mathbf{t} \cdot \mathbf{u} \, dS$$

is continuous over $W^{1,p}(\Omega, \mathbb{R}^3)$.

Finally let $\mathbf{u}_0 : \Gamma_0 \rightarrow \mathbb{R}^3$ be measurable and such that the set

$$U = \{\mathbf{u} \in W^{1,p}(\Omega, \mathbb{R}^3) : \text{Cof } \nabla \mathbf{u} \in L^q, \det \nabla \mathbf{u} \in L^r, \det \nabla \mathbf{u} > 0 \text{ a.e. in } \Omega, \mathbf{u} = \mathbf{u}_0 \text{ on } \Gamma_0\}$$

is not empty.

Then, defining the functional $\mathcal{F} : U \rightarrow \mathbb{R} \cup \{+\infty\}$ as

$$\mathcal{F}[\mathbf{u}] = \int_{\Omega} \Psi(\nabla \mathbf{u}) dV - L[\mathbf{u}]$$

and supposing that $\inf \mathcal{F}[\mathbf{u}] < +\infty$, there exists

$$\min_{\mathbf{u} \in U} \mathcal{F}[\mathbf{u}].$$

2.2 State of art of passive behaviour of muscle tissue

In this section we are going to introduce two of the most classical models for passive muscle tissue.

Let us begin by introducing the deformation gradient \mathbf{F}_λ , which in our case will be an uniaxial deformation along the muscle's fibers direction that we consider along $\mathbf{m} = \mathbf{e}_1$.

Let $\mathbf{M} = \mathbf{m} \otimes \mathbf{m}$ be the structural tensor, then the deformation gradient \mathbf{F}_λ will be

$$\mathbf{F}_\lambda = \lambda \mathbf{M} + \frac{1}{\sqrt{\lambda}} (\mathbf{I} - \mathbf{M})$$

and consequently

$$\mathbf{C} = \lambda^2 \mathbf{M} + \frac{1}{\lambda} (\mathbf{I} - \mathbf{M})$$

The incompressibility constraint is satisfied from the form of \mathbf{F}_λ , in fact we always have $J = 1$.

For the elastic energy we will take the following function of \mathbf{C} , used in [7]

$$\Psi(\mathbf{C}) = \frac{\mu}{4} \left\{ \frac{1}{\alpha} [e^{\alpha(I_p-1)} - 1] + \frac{1}{\beta} [e^{\beta(K_p-1)} - 1] \right\}$$

where I_p and K_p and called *generalized invariants*

$$I_p = \frac{w_0}{3} \text{tr } \mathbf{C} + (1 - w_0) \text{tr } \mathbf{C} \mathbf{M}$$

$$K_p = \frac{w_0}{3} \text{tr } \mathbf{C}^{-1} + (1 - w_0) \text{tr } \mathbf{C}^{-1} \mathbf{M}$$

The parameters $\alpha > 0$, $\beta > 0$ are dimensionless parameters that depend on the material, μ is an elastic parameter and w_0 is another dimensionless parameter which weighs the amount of isotropy and anisotropy of the material.

It's important to notice that if no deformation is applied to the body, that is $\mathbf{F}_\lambda = \mathbf{I}$

then $\Psi(\mathbf{I}) = 0$, that means that no force is exerted by the material. The generalized invariants can be rewritten in function of the invariants of \mathbf{C} , so that we can derive the first Piola-Kirchhoff tensor using (2.1).

$$I_p = \frac{w_0}{3}I_1 + (1 - w_0)I_4$$

$$K_p = \frac{w_0}{3} \frac{I_2}{I_3} + (1 - w_0) \frac{I_5 - I_1 I_4 + I_2}{I_3}$$

obtaining

$$\mathbf{P}(\mathbf{F}) = \frac{\mu}{2} \mathbf{F} \lambda \left\{ e^{\alpha(I_p-1)} \left[\frac{w_0}{3} \mathbf{I} + (1-w_0) \mathbf{M} \right] - e^{\beta(K_p-1)} \mathbf{C}^{-1} \left[\frac{w_0}{3} \mathbf{I} + (1-w_0) \mathbf{M} \right] \mathbf{C}^{-1} \right\} - p \mathbf{F}^{-T}$$

and which component along the \mathbf{m} direction is

$$P_{\mathbf{M}} = \mathbf{P} : \mathbf{M} = \frac{\mu}{2} \lambda \left\{ e^{\alpha(I_p-1)} \left[\frac{w_0}{3} + (1 - w_0) \right] - e^{\beta(K_p-1)} \left[\frac{w_0}{3} + (1 - w_0) \right] \lambda^{-4} \right\}$$

where $\mathbf{A} : \mathbf{B}$ is the matrix scalar product.

The generalized invariants considered as a function of λ are

$$I_p = \frac{w_0}{3} \left(\lambda^2 + \frac{2}{\lambda} \right) + (1 - w_0) \lambda^2$$

$$K_p = \frac{w_0}{3} \left(\frac{1}{\lambda^2} + 2\lambda \right) + (1 - w_0) \frac{1}{\lambda^2}$$

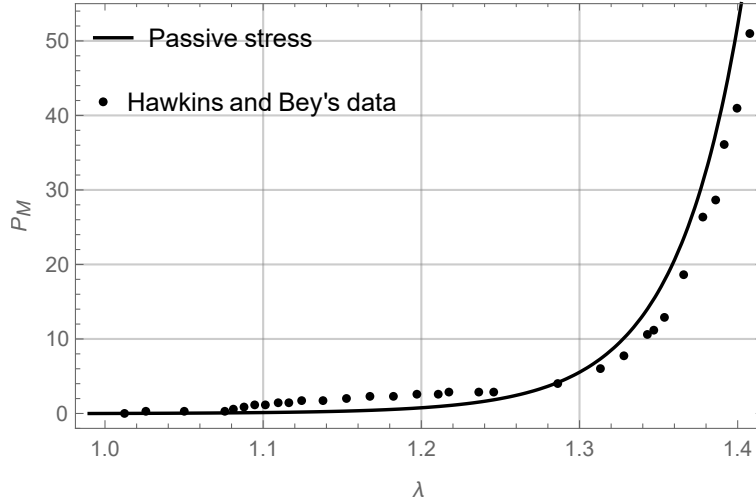


Figure 2.2: Exponential model's fit on Hawkins and Bey's data

Another model which should be taken in consideration is the energy used by Gent [5] to model rubber-like materials.

The elastic energy which we will use is

$$\Psi(\mathbf{C}) = -\frac{\mu}{2} I_{max} \log \left(1 - \frac{I_1 - 3}{I_{max}} \right)$$

which is fully isotropic.

In this model μ is the shear modulus, while I_{max} imposes the maximum value which can be reached by I_1 .

After some trivial calculations we can derive P_M as done before, obtaining

$$P_M = \mu \left(1 - \frac{\lambda^2 + 2\lambda^{-1} - 3}{I_{max}} \right)^{-1} (\lambda - \lambda^{-1})$$

from which we get the following result

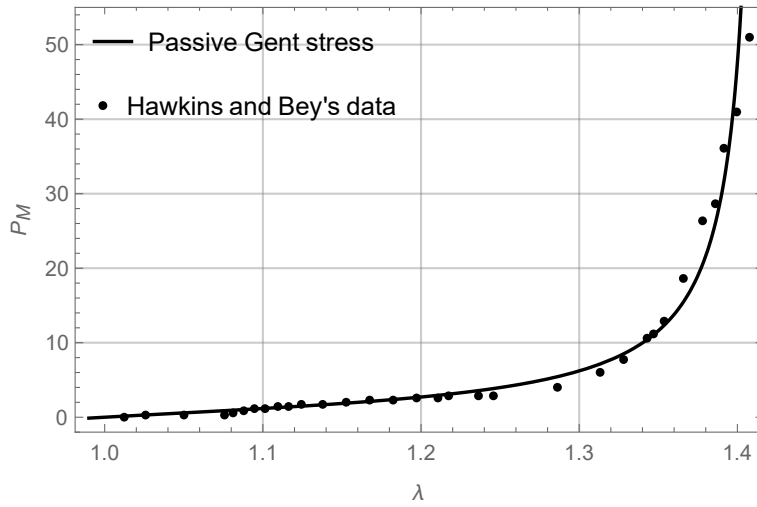


Figure 2.3: Gent model's fit on Hawkins and Bey's data

Gent's elastic energy is simpler, since it depends on only two parameters, and has the advantage of having an asymptote, which could physically represent the limits of the model, in fact it could represent the rupture of the tissue due to excessive elongation. Moreover a Gent material acts as a Neo-Hookean material for small strains.

Chapter 3

Active Stress vs Active Strain approaches

There is a category of soft materials, called active materials, which can deform under external stimuli (typically chemical or electrical) without any external load. Muscle tissue is a typical example of these materials, in fact an electrical stimulus leads the fibers to a contraction. In the following sections we will introduce two methods to describe the activation of the tissue: the active stress and the active strain. These methods take advantage of a decomposition, either additive for the energy or multiplicative for the deformation gradient, which make it possible to distinguish between an activated and non-activated state of the material. Moreover we will see how these methods affect the mathematical properties of the energy, to ensure that the problem can be well-posed.

3.1 The active stress approach

This approach, called *active stress approach* consist in the additive decomposition of the strain energy function as the sum of two parts which describe the passive and the active behaviour of the material.

$$\Psi(\mathbf{F}) = \Psi_{pass}(\mathbf{F}) + \Psi_{act}(\mathbf{F})$$

where $\Psi_{pass}(\mathbf{F})$ represents the passive energy and $\Psi_{act}(\mathbf{F})$ the active energy. The first Piola-Kirchhoff stress tensor is obtained in the following way:

$$\mathbf{P}(\mathbf{F}) = \mathbf{P}_{pass}(\mathbf{F}) + \mathbf{P}_{act}(\mathbf{F}) = \frac{\partial \Psi_{pass}}{\partial \mathbf{F}}(\mathbf{F}) + \frac{\partial \Psi_{act}}{\partial \mathbf{F}}(\mathbf{F}) - p\mathbf{F}^{-T}$$

where $\mathbf{P}_{act}(\mathbf{F})$ is the stress given by the activation.

For the passive part, which is already discussed above, we will consider a Gent material.

Since the deformation we are considering is \mathbf{F}_λ and the fibers, the active part of the material, are transversely isotropic and are deformed along the direction $\mathbf{m} = \mathbf{e}_1$, we will consider Ψ_{act} as a function of I_4 , in particular as a function of its square root, which in this case is exactly λ , in fact

$$I_4 = \text{tr } \mathbf{CM} = \lambda^2$$

Now since the active part of the energy is written in terms of $\sqrt{I_4}$, the stress relative to the active part will be obtained as follows:

$$\mathbf{P}_{act}(\mathbf{F}) = 2 \frac{\partial \Psi}{\partial \mathbf{F}}(\sqrt{I_4}) \mathbf{Fm} \otimes \mathbf{Fm} := P_{act}(\sqrt{I_4}) \mathbf{Fm} \otimes \mathbf{Fm}$$

We are going to choose the P_{act} used in [8], which is the following:

$$P_{act}(\lambda) = \begin{cases} P_{opt} \frac{\lambda_{min} - \lambda}{\lambda_{min} - \lambda_{opt}} \exp \frac{(2\lambda_{min} - \lambda - \lambda_{opt})(\lambda - \lambda_{opt})}{2(\lambda_{min} - \lambda_{opt})^2}, & \lambda > \lambda_{min} \\ 0, & \text{otherwise} \end{cases}$$

from which the following active part of the energy is obtained:

$$\Psi_{act}(\lambda) = \begin{cases} P_{opt}(\lambda_{min} - \lambda_{opt}) \left[\exp \frac{(2\lambda_{min} - \lambda - \lambda_{opt})(\lambda - \lambda_{opt})}{2(\lambda_{min} - \lambda_{opt})^2} - e^{\frac{1}{2}} \right], & \lambda > \lambda_{min} \\ 0, & \text{otherwise} \end{cases}$$

By using least square optimization the following parameters are obtained:

- $P_{opt} = 73.52kPa$, this parameter describes the maximal activation obtained
- $\lambda_{min} = 0.682$, which is the minimal length for activation
- $\lambda_{opt} = 1.192$, that describes the point of maximum

The curve in Fig 3.1 is obtained, and we can notice that for $\lambda < 0.9$ and for $1 < \lambda < 1.3$ the fit is not good, but the curves have a similar shape.

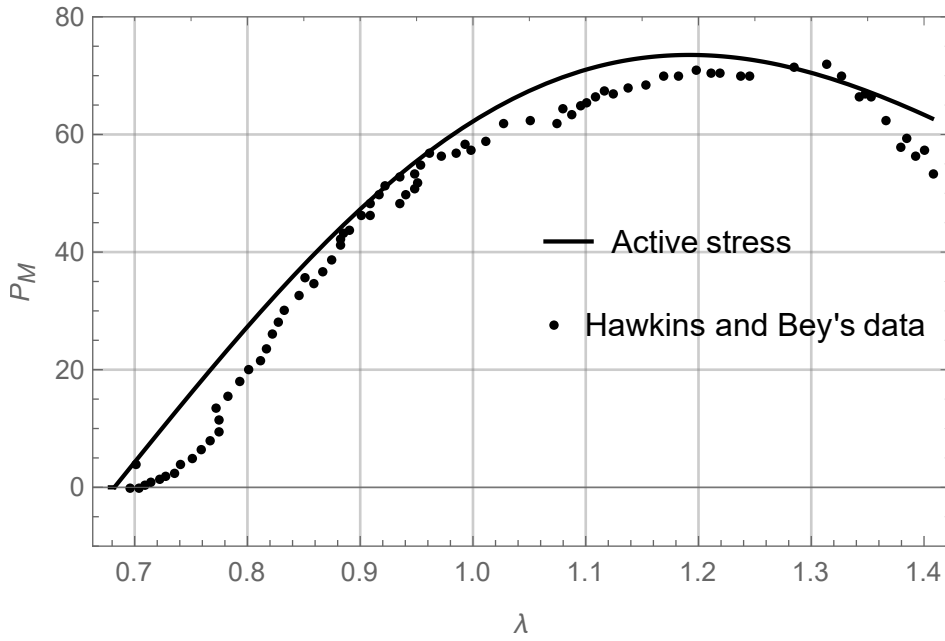


Figure 3.1: Active stress along fibers and Hawkins and Bey's active data

Now we can compute the total stress along the fibers:

$$P_{\mathbf{M}}(\lambda) = \mathbf{P} \cdot \mathbf{M} = \mu \left(1 - \frac{\lambda^2 + 2\lambda^{-1} - 3}{I_{max}}\right)^{-1} (\lambda - \lambda^{-1}) + \mathbf{P}_{act}(\lambda)$$

where $\mu = 4$ and $I_{max} = 0.42$.

The result obtained is the following:

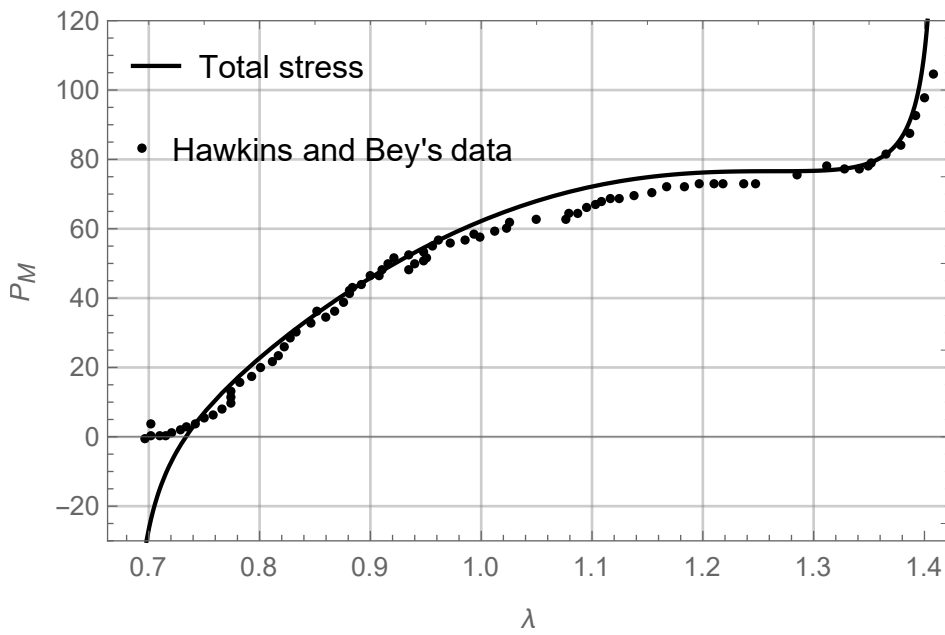


Figure 3.2: Gent's model fit on Hawkins and Bey's data

we can see that the behaviour of the curve almost fully respects the data by Hawkins and Bey [4], but for the intervals where the active curve didn't fit well. The last concern about this method is about the mathematical properties which ensure the well-posedness of the problem. Thanks to the fact the the decomposition is additive, we can say that the total energy inherits the properties of the "weaker" energy, for example if the active energy is rank-one convex, and the passive energy is polyconvex, the total energy will be only rank-one convex. In our case the active energy may not be polyconvex.

3.2 The active strain approach

In this model, called *active strain approach*, we consider a multiplicative decomposition of the deformation gradient.

Considering the Kröner-Lee decomposition, which is

$$\mathbf{F} = \mathbf{F}_e \mathbf{F}_a$$

where \mathbf{F}_e is the elastic strain, the part which contributes to elastic energy and \mathbf{F}_a represents the deformation gradient given by the activation.

This decomposition represents that the fiber's contraction can be physically interpreted as a geometrical remodeling of the body structure on a microscopic level.

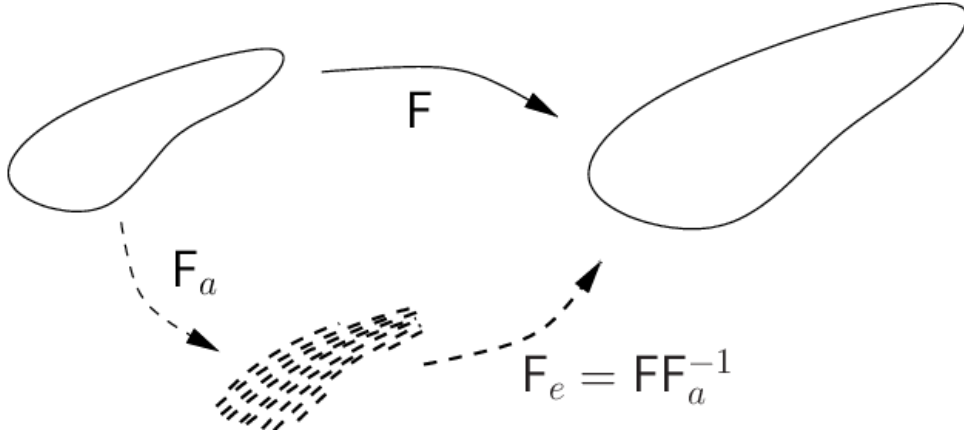


Figure 3.3: Kröner-Lee decomposition

We can rewrite the strain energy as

$$\Psi(\mathbf{F}; \mathbf{F}_a) = \det(\mathbf{F}_a) \Psi_{pass}(\mathbf{F}\mathbf{F}_a^{-1}) \quad (3.1)$$

and the first Piola-Kirchhoff tensor writes as

$$\mathbf{P}(\mathbf{F}; \mathbf{F}_a) = \det(\mathbf{F}_a) \frac{\partial \Psi_{pass}}{\partial \mathbf{F}}(\mathbf{F}\mathbf{F}_a^{-1}) - p\mathbf{F}^{-T}$$

From now on we are going to follow the work done in [6], which uses a simplified version of the exponential energy to model the passive behaviour, then activates it with a non-constant activation parameter.

The strain energy density used is

$$\Psi_{pass}(\mathbf{F}) = \frac{\mu}{4} \left\{ \frac{1}{\alpha} [e^{\alpha(I_p-1)} - 1] + K_p - 1 \right\}$$

where, as seen in the past chapter,

$$I_p = \frac{w_0}{3} \text{tr } \mathbf{C} + (1 - w_0) \text{tr } \mathbf{C} \mathbf{M}$$

$$K_p = \frac{w_0}{3} \text{tr } \mathbf{C}^{-1} + (1 - w_0) \text{tr } \mathbf{C}^{-1} \mathbf{M}$$

and the parameters have the same meaning as the energy described before.

The first Piola-Kirchhoff stress tensor then will be given by

$$\mathbf{P}_{pass}(\mathbf{F}) = \frac{\mu}{2} \mathbf{F} \left\{ e^{\alpha(I_p-1)} \left[\frac{w_0}{3} \mathbf{I} + (1 - w_0) \mathbf{M} \right] - \mathbf{C}^{-1} \left[\frac{w_0}{3} \mathbf{I} + (1 - w_0) \mathbf{M} \right] \mathbf{C}^{-1} \right\} - p \mathbf{F}^{-T}$$

Using $\mu = 0.1599 \text{ kPa}$, $\alpha = 19.35$ and $w_0 = 0.7335$, the following result for the passive behaviour of the muscle can be obtained.

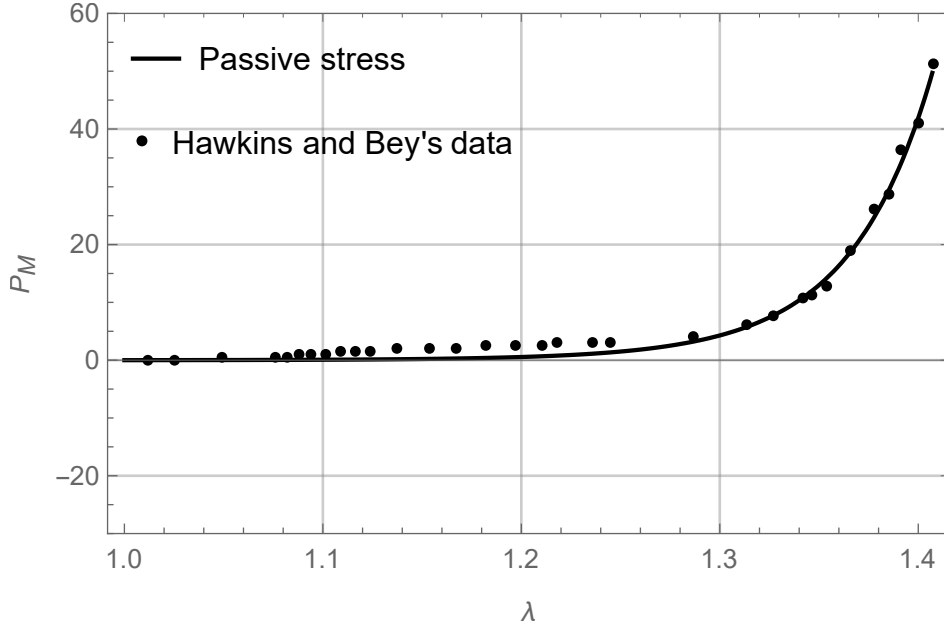


Figure 3.4: Passive stress along fibers and Hawkins and Bey's active data

Now we want to activate the muscle, and to do this we need to define \mathbf{F}_a . The chosen form is the following

$$\mathbf{F}_a = (1 - a) \mathbf{m} \otimes \mathbf{m} + \frac{1}{\sqrt{1 - a}} (I - \mathbf{m} \otimes \mathbf{m})$$

where a is such that $0 \leq a < 1$ and it's a dimensionless parameter which describes the activation of the muscles, where $a = 0$ means that the muscle isn't activated. Moreover we have that $\det \mathbf{F}_a = 1$. The parameter a could be considered constant, in order to have a simpler model, but we can show that in this case it will not fit well the experimental data.

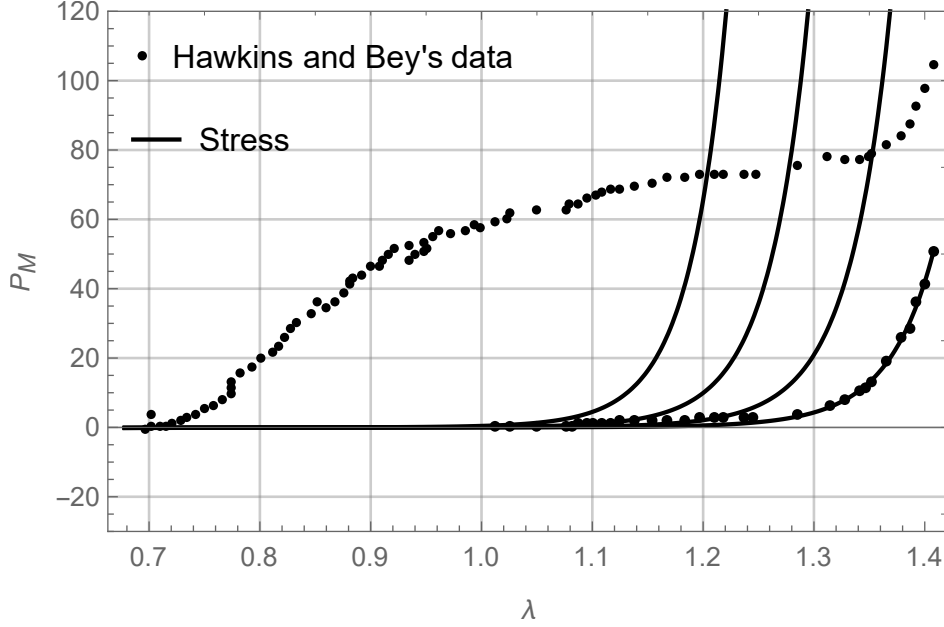


Figure 3.5: Activation behaviour with respect to λ , with γ constant, $\gamma = 0.05, 0.1, 0.15$

This choice of activation is given by the fact that in the active part of the experimental data the stress-stretch relationship reaches a maximum before decreasing, which suggests that there is a behaviour dictated at the molecular level for which the activation a of the muscle tissue depends on the stretch λ .

In particular we will consider $a = a(I_4)$, where I_4 is the fourth invariant, and represents the squared stretch along the fibers.

A consequence of this assumption is that $\mathbf{F}_a = \mathbf{F}_a(I_4)$, and this leads to the following activated form of the first Piola-Kirchhoff stress tensor:

$$\mathbf{P}(\mathbf{F}) = 2\mathbf{F} \frac{\partial \Psi}{\partial \mathbf{C}} - \hat{p} \mathbf{F}^{-T} = 2\mathbf{F} \frac{\partial}{\partial \mathbf{C}} [\Psi_{pass}(\mathbf{F}_a^{-T}(I_4) \mathbf{C} \mathbf{F}_a^{-1}(I_4))] - \hat{p} \mathbf{F}^{-T}$$

From (3.1) we find the energy:

$$\Psi = \Psi_{pass}(\mathbf{F}_\lambda \mathbf{F}_a^{-1}) = \Psi(\lambda, a(\lambda)) = \frac{\mu}{4} \left[\frac{1}{\alpha} (e^{\alpha(I_p-1)} - 1) + K_p - 1 \right]$$

where now, considering

$$\mathbf{C}_e = \frac{\lambda^2}{(1-a)^2} \mathbf{m} \otimes \mathbf{m} + \frac{1-a}{\lambda} (I - \mathbf{m} \otimes \mathbf{m})$$

we have that

$$I_p = \frac{w_0}{3} \text{tr } \mathbf{C}_e + (1 - w_0) \text{tr } \mathbf{C}_e \mathbf{M} = \left(1 - \frac{2}{3}w_0\right) \frac{\lambda^2}{(1-a)^2} + \frac{2w_0(1-a)}{3\lambda}$$

$$K_p = \frac{w_0}{3} \text{tr } \mathbf{C}_e^{-1} + (1 - w_0) \text{tr } \mathbf{C}_e^{-1} \mathbf{M} = \left(1 - \frac{2}{3}w_0\right) \frac{(1-a)^2}{\lambda^2} + \frac{2w_0}{3} \frac{\lambda}{(1-a)}$$

Now we have to find the expression of $a(\lambda)$, which has to satisfy the equation

$$P_{tot} = P_{pas} + P_{act} \quad (3.2)$$

in which we can find P_{tot} and P_{pas} from the strain energy densities, with the condition that $a(\lambda_{min}) = 0$, with $\lambda_{min} = 0.6$, then P_{act} has to be modeled from the data. By integrating equation (3.2) we find that

$$\Psi(\lambda, a(\lambda)) - \Psi(\lambda, 0) = S_{act} \quad (3.3)$$

with S_{act} is obtained by integrating P_{act} , considering $S_{act}(\lambda_{min}) = 0$.

To simplify we are going to take

$$a(\lambda) = e^{-p_6\lambda}(p_5\lambda^5 + p_4\lambda^4 + p_3\lambda^3 + p_2\lambda^2 + p_1\lambda + p_0)(\lambda - \lambda_{min})$$

and find it by using least square optimization on (3.3), where S_{act} has been found using the trapezoidal rule on the active data.

The form of the activation will be the following

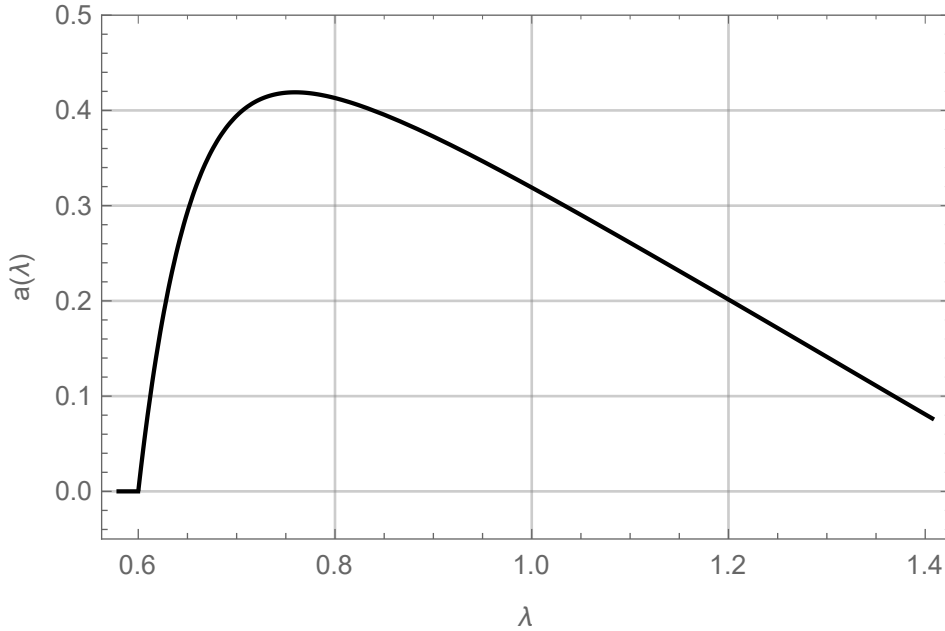


Figure 3.6: Activation behaviour with respect to λ

where the function has been truncated to prevent physical anomalies, like the total stress becoming less than the passive one.

Finally we can compute the total stress along \mathbf{m} , obtaining the following result

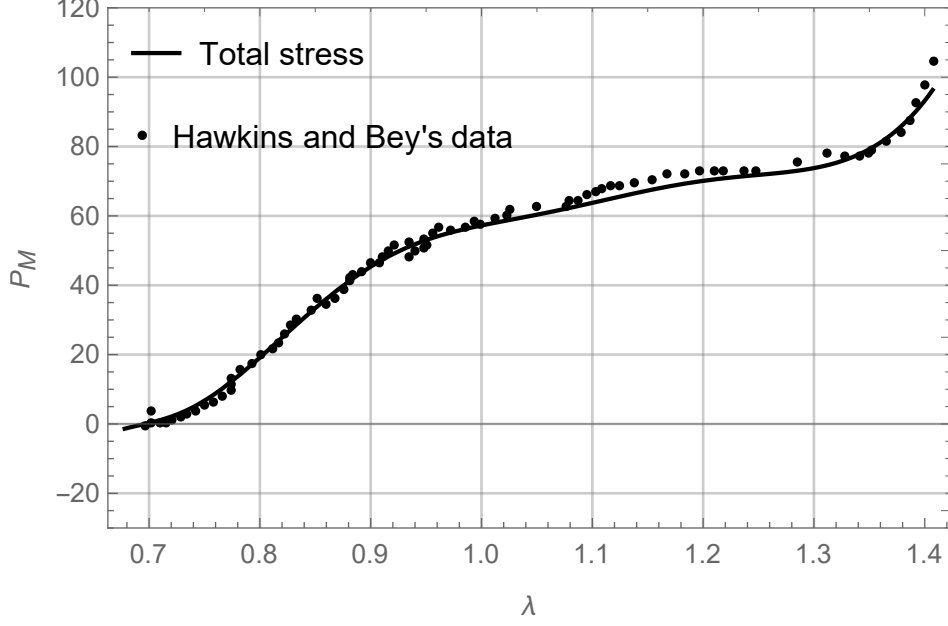


Figure 3.7: Total stress-strain relation and Hawkins and Bey's data

In the case of active strain, there is a trade off between activation complexity and mathematical properties of the total energy, if the activation \mathbf{F}_a is constant, the total energy will preserve the convexity properties of the passive energy, $\forall \mathbf{H} \neq 0$, we have that

$$\mathbf{H} : \frac{\partial^2 \Psi}{\partial \mathbf{F} \partial \mathbf{F}} : \mathbf{H} = \mathbf{H} : \left(\frac{\partial^2}{\partial \mathbf{F} \partial \mathbf{F}} \Psi(\mathbf{F} \mathbf{F}_a^{-1}) \right) : \mathbf{H} = \mathbf{H} \mathbf{F}_a^{-1} : \frac{\partial^2 \Psi}{\partial \mathbf{F} \partial \mathbf{F}} : \mathbf{H} \mathbf{F}_a^{-1} > 0$$

and if \mathbf{H} is a rank-one tensor, also $\mathbf{H} \mathbf{F}_a^{-1}$ is rank-one convex, so the total energy preserves the properties of the passive one.

For what concerns the polyconvexity of the function we refer to the work by Neff [13], in particular to the Lemma 6.5 :

Lemma. *Let $\Psi(\mathbf{F})$ be polyconvex and assume that $\mathbf{F}_a \in L^\infty(\Omega, GL^+(3, \mathbb{R}))$, where*

$$GL^+(3, \mathbb{R}) := \left\{ \mathbf{X} \in M^{3 \times 3} \mid \det \mathbf{X} > 0 \right\},$$

is given. Then the function

$$\hat{\Psi}(x, \mathbf{F}) := \Psi(\mathbf{F} \mathbf{F}_a^{-1}(x)) \det \mathbf{F}_a(x)$$

is itself polyconvex.

However if we take a more complicated $\mathbf{F}_a(\mathbf{F})$, the mathematical properties of the passive energy may be lost with activation.

Chapter 4

A novel multiphase model with active strain

In this chapter we will use the method used in the work by Riccobelli and Ambrosi [1], the mixture active strain. This model considers an additive decomposition in an isotropic and an anisotropic part, and uses the Kröner-Lee decomposition of the deformation gradient only in the anisotropic part.

4.1 The mixture active strain approach

Another way to model muscle tissue is the mixture active strain approach, which is a really interesting method, because by decomposing the energy in the sum of an isotropic and an anisotropic part, we can model the passive behaviour of the material, and activate, by applying the active strain approach, only the anisotropic part of the material, which represents the fibers. So, even if this is a particular case of the active stress, we can think of this as a more physiologically accurate way to represent muscle tissue.

The energy will have the following form, which is the one shown above for fiber-reinforced materials.

$$\Psi(\mathbf{F}) = \Psi_{iso}(\mathbf{F}) + \Psi_{ani}(I_4, I_5) \quad (4.1)$$

From (4.1) we can derive the Piola-Kirchhoff stress tensor, which reads

$$\mathbf{P}_{pass}(\mathbf{F}) = \frac{\partial \Psi_{iso}}{\partial \mathbf{F}} + \det(\mathbf{F}_a) \frac{\partial \Psi_{ani}}{\partial \mathbf{F}} - p \mathbf{F}^{-T}$$

Now, since only the anisotropic part of the energy will activate, we will apply the Kröner-Lee decomposition only on it.

$$\mathbf{F} = \mathbf{F}_e \mathbf{F}_a$$

So the total energy will read

$$\Psi = \Psi_{iso}(\mathbf{F}) + \det(\mathbf{F}_a) \Psi_{ani}(\mathbf{F}_e) = \Psi_{iso}(\mathbf{F}) + \det(\mathbf{F}_a) \Psi_{ani}(\mathbf{F} \mathbf{F}_a^{-1})$$

And the total stress derived will be

$$\mathbf{P}(\mathbf{F}) = \frac{\partial \Psi}{\partial \mathbf{F}} = \frac{\partial \Psi_{iso}}{\partial \mathbf{F}} + \det(\mathbf{F}_a) \frac{\partial \Psi_{ani}(\mathbf{F}\mathbf{F}_a^{-1})}{\partial \mathbf{F}} - p\mathbf{F}^{-T} = \mathbf{P}_{iso}(\mathbf{F}) + \mathbf{P}_{ani}(\mathbf{F}\mathbf{F}_a^{-1})\mathbf{F}_a^{-T} - p\mathbf{F}^{-T}$$

In (4.1) the isotropic part of the material is described as a Gent material, so that the strain energy density will be given by

$$\Psi_{iso} = -\frac{\mu}{2} I_{max} \log \left(1 - \frac{I_1 - 3}{I_{max}} \right)$$

where I_1 is the first invariant of \mathbf{C} , μ is the shear modulus and I_{max} is the maximum value of I_1 . The anisotropic part considered in (4.1) is

$$\Psi_{ani} = \alpha \beta (I_4^{\frac{1}{2\beta}} - 1)^2$$

where α and β are material constants. This energy is usually used with the square root of I_4 , but in this case a parameter β is considered to take into account the change of convexity.

For what concerns the deformation gradient and its Kröner-Lee decomposition we have an uniaxial deformation in the direction \mathbf{m} , as shown in the previous chapters

$$\mathbf{F} = \mathbf{F}_\lambda = \lambda \mathbf{M} + \frac{1}{\sqrt{\lambda}} (\mathbf{I} - \mathbf{M})$$

where $\mathbf{m} = \mathbf{e}_1$ and $\mathbf{M} = \mathbf{m} \otimes \mathbf{m}$, and

$$\mathbf{F}_a = (1 - \gamma) \mathbf{M} + \frac{1}{\sqrt{1 - \gamma}} (\mathbf{I} - \mathbf{M})$$

where γ represents the shortening of the fibers. In this model we will consider the activation parameter γ to be constant. This choice will, on one side, simplify the model, but on the other side remove some degrees of freedom with respect to the activation seen above.

Since $\det \mathbf{F}_a = 1$, the first Piola-Kirchhoff stress tensor will be given by

$$\mathbf{P}(\mathbf{F}) = \mathbf{P}_{iso}(\mathbf{F}) + \mathbf{P}_{ani}(\mathbf{F}\mathbf{F}_a^{-1})\mathbf{F}_a^{-T} - p\mathbf{F}^{-T}$$

and in particular, considering the energies chosen above, we have

$$\begin{aligned} \mathbf{P}_{iso}(\mathbf{F}) &= \frac{\partial \Psi_{iso}}{\partial \mathbf{F}} = \mu \left(1 - \frac{I_1 - 3}{I_{max}} \right)^{-1} \mathbf{F} \\ \mathbf{P}_{ani}(\mathbf{F}) &= \frac{\partial \Psi_{ani}}{\partial \mathbf{F}} = 2\alpha \frac{I_4^{\frac{1}{2\beta}} - 1}{I_4^{\frac{2\beta-1}{2\beta}}} \mathbf{F}\mathbf{M} \end{aligned}$$

Now what we are interested in is the principal stress in the direction \mathbf{m} , which we'll call $P_{\mathbf{M}}$ and which it's obtained by differentiating $\Psi(\mathbf{F}_\lambda)$ with respect to λ :

$$P_{\mathbf{M}}(\lambda, \gamma) = \frac{d\Psi(\mathbf{F}_\lambda)}{d\lambda}$$

In our case we will have that, using the mixture active strain approach, the first Piola-Kirchhoff stress tensor will be decomposed as

$$P_{\mathbf{M}}(\lambda, \gamma) = P_{\mathbf{M}}^{iso}(\lambda) + P_{\mathbf{M}}^{ani}(\lambda, \gamma)$$

where

$$P_{\mathbf{M}}^{iso}(\lambda) = \frac{d\Psi_{iso}(\mathbf{F}_\lambda)}{d\lambda}$$

$$P_{\mathbf{M}}^{ani}(\lambda, \gamma) = \frac{d\Psi_{ani}(\mathbf{F}_\lambda \mathbf{F}_a^{-1})}{d\lambda}$$

and considering the form of the energies shown before, we get:

$$P_{\mathbf{M}}^{iso}(\lambda) = \mu \left(1 - \frac{\lambda^2 + 2\lambda^{-1} - 3}{I_{max}} \right)^{-1} (\lambda - \lambda^{-1})$$

$$P_{\mathbf{M}}^{ani}(\lambda, \gamma) = 2\alpha \left(\left(\frac{\lambda}{1-\gamma} \right)^{\frac{1}{\beta}} \right) \left(\left(\frac{\lambda}{1-\gamma} \right)^{\frac{1}{\beta}} - 1 \right) \lambda^{-1}$$

and finally

$$P_{\mathbf{M}}(\lambda, \gamma) = \mu \left(1 - \frac{\lambda^2 + 2\lambda^{-1} - 3}{I_{max}} \right)^{-1} (\lambda - \lambda^{-1})$$

$$+ 2\alpha \left(\left(\frac{\lambda}{1-\gamma} \right)^{\frac{1}{\beta}} \right) \left(\left(\frac{\lambda}{1-\gamma} \right)^{\frac{1}{\beta}} - 1 \right) \lambda^{-1}$$

The following result is obtained:

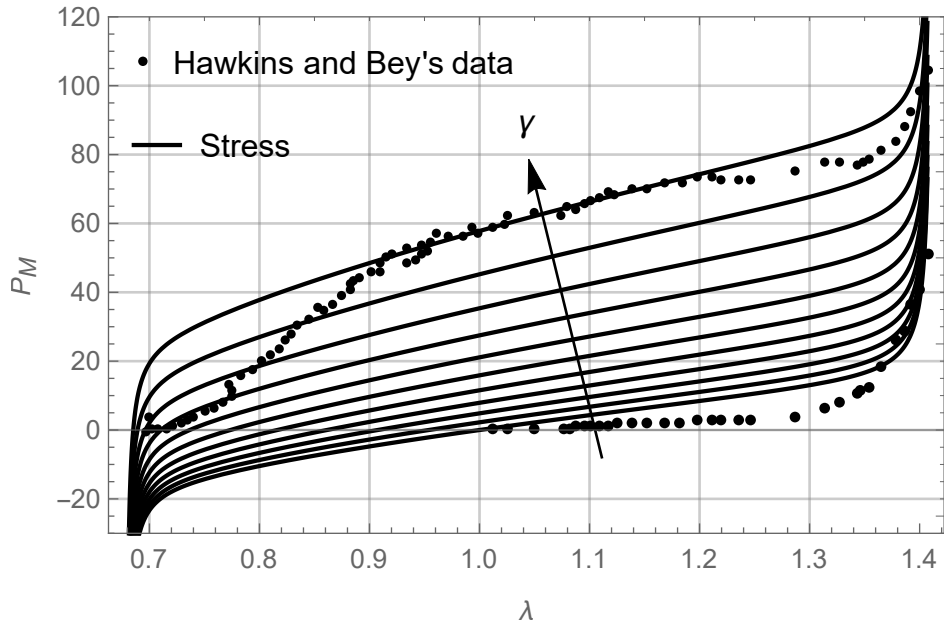


Figure 4.1: Plot of P_M when $\mu = 1.8kPa$, $I_{max} = 0.41$, $\alpha = 31kPa$, $\beta = 1.5$ and γ varies from 0 to 0.5 with steps of 0.05.

The curve is in good agreement with the data for $\gamma = 0.5$, which is also an acceptable value for the physiological shortening of the fibers.

As we can see above the passive curve doesn't represent the experimental data very well, and the total curve shows a good agreement with the data only between $\lambda = 0.9$ and $\lambda = 1.2$.

To better understand the contribution of the components we can see the contribution of the anisotropic component and how it changes with the activation of the material, while the contribution of the isotropic component was already shown in Chapter 2.

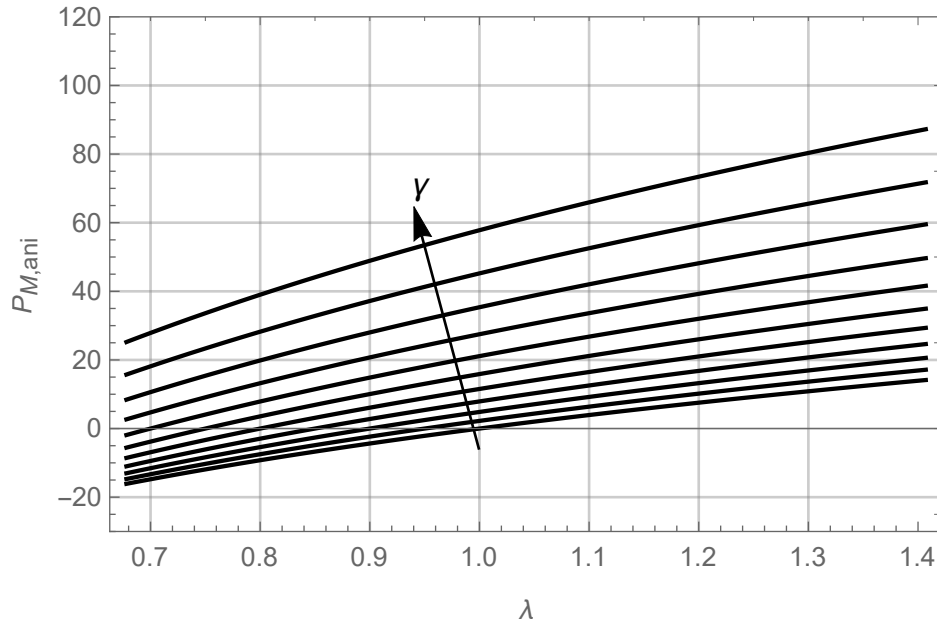


Figure 4.2: Plot of the anisotropic component where γ varies from 0 to 0.5 with steps of 0.05.

We can see better the limitations of this model by looking only at its active part.

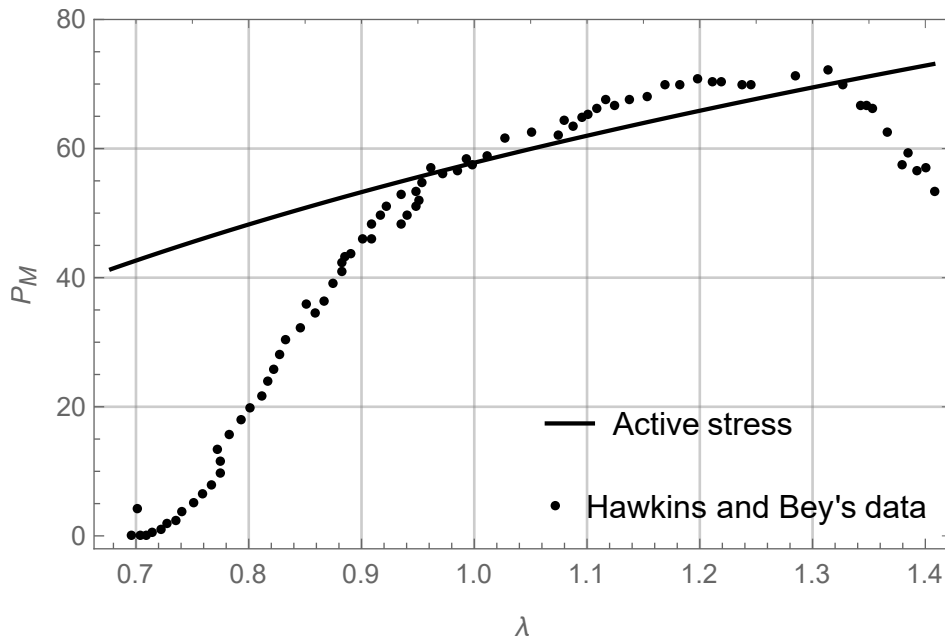


Figure 4.3: Active contribution of the model and active experimental data.

We can observe that in the active case the curve doesn't represent the behaviour of the data, still being a good approximation for some λ in the middle range.

For what concerns the mathematical issues raised by the mixture active strain approach, if both Ψ_{iso} and Ψ_{ani} are rank-one convex and \mathbf{F}_γ is constant, then:

$$\mathbf{H} : \frac{\partial^2 \Psi}{\partial \mathbf{F} \partial \mathbf{F}} : \mathbf{H} = \mathbf{H} : \frac{\partial^2 \Psi_{iso}(\mathbf{F})}{\partial \mathbf{F} \partial \mathbf{F}} : \mathbf{H} + \mathbf{H} \mathbf{F}_\gamma^{-1} : \frac{\partial^2 \Psi_{ani}(\mathbf{F})}{\partial \mathbf{F} \partial \mathbf{F}} : \mathbf{H} \mathbf{F}_\gamma^{-1} > 0$$

for all \mathbf{H} rank-one convex.

For polyconvexity we have the same condition, in fact if both Ψ_{iso} and Ψ_{ani} are polyconvex then the activated energy is polyconvex too, as a direct consequence of the result by Neff [13], already shown in Chapter 3.

4.2 Anisotropy and representation by invariants

In this chapter we are going to briefly resume the work done by Murphy in [3], since it regards the choice of the dependence of the anisotropic part of the energy on I_4 and I_5 .

We start by setting in the general framework proposed by Weiss in [21] to model a transversely isotropic tissue, which is

$$\Psi = F_1(I_1, I_2) + F_2(I_4) + F_3(I_1, I_2, I_4) = \Psi(I_1, I_2, I_4) \quad (4.2)$$

where

- Ψ_1 is the energy contribution by the anisotropic part of the tissue
- Ψ_2 represents the contribution of the anisotropic part
- Ψ_3 represents the interaction between the collagen matrix and the fibers

In this subsection (4.2), to keep the notation of the work done by Murphy, we will use the following invariants I_1 , I_2 and I_3 :

$$\begin{aligned} I_1 &= \text{tr } \mathbf{B} \\ I_2 &= \frac{1}{2} [I_1^2 - \text{tr } \mathbf{B}^2] \\ I_3 &= \det \mathbf{B} = J^2 \end{aligned}$$

What we want to show now is that the form of the energy in (4.2) is not physically realistic.

We start by taking the Cauchy stress for an incompressible, homogeneous, transversely isotropic, non-linear hyperelastic material, whose energy is dependent on both anisotropic invariants I_4 and I_5 , given by

$$\mathbf{t} = -p\mathbf{I} + 2\Psi_1\mathbf{B} + 2\Psi_2(I_1\mathbf{B} - \mathbf{B}^2) + 2\Psi_4\mathbf{Fm} \otimes \mathbf{Fm} + 2\Psi_5(\mathbf{Fm} \otimes \mathbf{BFm} + \mathbf{BFm} \otimes \mathbf{Fm})$$

where \mathbf{m} is the preferential direction, $\Psi_k = \frac{\partial \Psi}{\partial I_k}$, with $k = 1, \dots, 5$ and p is an arbitrary pressure.

The first two conditions required on the energy are the ones that ensure that there is no stress in the undeformed configuration, and these are:

$$2\Psi_1^0 + 4\Psi_2^0 = p^0 \quad (4.3)$$

$$\Psi_4^0 + 2\Psi_5^0 = 0 \quad (4.4)$$

where the 0 superscript means that is evaluated in the undeformed configuration, and the two conditions are given by the fact that \mathbf{m} is arbitrary.

Lastly we want the whole energy to be null in the undeformed configuration:

$$\Psi^0 = 0$$

Now we set in the framework of linear elasticity (see, for example, Gurtin [12],), assuming that we have infinitesimal strains. Assuming that the preferential direction $\mathbf{m} = \mathbf{e}_3$ and assuming that the strain tensor has component ϵ_{ij} we have that

$$\mathbf{t}_{11} = -p + 2\mu_T \epsilon_{11}$$

$$\mathbf{t}_{22} = -p + 2\mu_T \epsilon_{22}$$

$$\mathbf{t}_{33} = -p + C_{33} \epsilon_{33}$$

$$\mathbf{t}_{23} = 2\mu_L \epsilon_{23}$$

$$\mathbf{t}_{13} = 2\mu_L \epsilon_{13}$$

$$\mathbf{t}_{12} = 2\mu_T \epsilon_{12}$$

where μ_T is the infinitesimal shear along the plane normal to the fibers, μ_L the infinitesimal shear along the fibers and C_{33} a material constant.

Starting from this, Merodio and Ogden in [20], in order to make linear and non-linear theory compatible, obtained some restrictions on the possible energies, which in terms of the constants used above are:

$$2\Psi_1^0 + 2\Psi_2^0 = \mu_T \quad (4.5)$$

$$2\Psi_1^0 + 2\Psi_2^0 + 2\Psi_5^0 = \mu_L \quad (4.6)$$

$$4\Psi_{44}^0 + 16\Psi_{45}^0 + 16\Psi_{55}^0 = E_L + \mu_T - 4\mu_L \quad (4.7)$$

where E_L is the Young's modulus in the direction along the fibers.

Now (4.6), using (4.5), can be rewritten as follows

$$2\Psi_5^0 = \mu_L - \mu_T \quad (4.8)$$

which, using (4.4) implies that

$$\Psi_4^0 = \mu_T - \mu_L \quad (4.9)$$

Now if we consider our material independent of I_5 we will have that $\Psi_5 = 0$, which implies in particular that $\Psi_5^0 = 0$ and from (4.9) we get

$$\mu_T = \mu_L \quad (4.10)$$

which means that the infinitesimal shear moduli perpendicular to the fibers and along them are identical.

This is a very counter-intuitive condition for a transversely isotropic material and, as we will see, it's not supported by experimental data.

The following studies are the ones cited in the work by Murphy:

- Sinkus et al. [22] using MR-Elastography on beef muscle, and two patients with breast lesions showed $1.5 < \mu_L/\mu_T < 2.2$.
- Genisson et al. [23] using transient elastography techniques on beef muscle and human biceps found $7.8 < \mu_L/\mu_T < 16$.
- Arbogast and Margulies [24] using oscillatory shear tests on porcine brainstem tissue found that $\mu_L > \mu_T$ for all strains investigated.
- Kruse et al. [25] using MR-Elastography on bovine semitendinosus skeletal muscle tissue found that $\mu_L > \mu_T$
- Kriz and Stinchcomb [26] using ultrasound found $\mu_L/\mu_T = 1.97$ for graphite-epoxy fibre-reinforced materials.
- Morrow et al. [27] is the only study in contrast with others, in which, testing the *extensor digitorum longus* muscle tissues from rabbits, obtained $\mu_L/\mu_T = 0.66$, but this study still shows that $\mu_L \neq \mu_T$.

Therefore there is experimental evidence that $\mu_L > \mu_T$ and even more that $\mu_L \neq \mu_T$, therefore (5.9) cannot be considered valid.

Next we want to investigate the non-linear response to shear on a transversely isotropic cube, with preferential direction $\mathbf{m} = \mathbf{e}_3$ as before. The block will be sheared using the following transformations:

Shear along the fibers: longitudinal shearing

1. $x = X, y = Y, z = Z + \kappa X$
2. $x = X, y = Y, z = Z + \kappa Y$

Shear across the fibers: perpendicular shear

3. $x = X, y = Y + \kappa Z, z = Z$
4. $x = X + \kappa Z, y = Y, z = Z$

Shear in planes normal to the fibers: transverse shear

5. $x = X, y = Y + \kappa X, z = Z$
6. $x = X + \kappa Y, y = Y, z = Z$

In an hyperelastic framework the three shears can be summarized as

$$\sigma = \frac{d\Psi(I_1(\kappa), I_2(\kappa), I_4(\kappa), I_5(\kappa))}{d\kappa}$$

and for the various shears:

Longitudinal shear:

$$I_1 = I_2 = 3 + \kappa^2, I_4 = 1, I_5 = 1 + \kappa^2$$

$$\sigma_L = 2\kappa(\Psi_1 + \Psi_2 + \Psi_5)$$

Perpendicular shear:

$$I_1 = I_2 = 3 + \kappa^2, I_4 = 1 + \kappa^2, I_5 = (1 + \kappa^2)^2 + \kappa^2$$

$$\sigma_P = 2\kappa(\Psi_1 + \Psi_2 + \Psi_4 + \Psi_5(3 + 2\kappa^2))$$

Transverse shear:

$$I_1 = I_2 = 3 + \kappa^2, I_4 = 1, I_5 = 1$$

$$\sigma_T = 2\kappa(\Psi_1 + \Psi_2)$$

Now if we consider $\Psi = \Psi(I_1, I_2, I_4)$, so that the energy doesn't depend on I_5 , we obtain that

$$\sigma_L = \sigma_T$$

which means that the longitudinal and transverse shear are the same for all shears. This is physically counter-intuitive for a transversely isotropic material, and there is some experimental evidence, like Dokos et al. [28] suggesting that the three shear responses are different from each other.

4.3 Results of proposed models: prediction on experimental data

In this section we will select some anisotropic energies from the work of Chagnon et al. [2], which depend only on both invariants I_4 and I_5 .

As shown above the fit on the Hawkins and Bey's data can be improved, so in the next table there are the energies selected from the work by Chagnon et al. [2], which can be used in the mixture active strain approach in order to obtain a better fit.

For what concerns the isotropic part of the model, we will use, as in Ch. 4.1, a Gent energy:

$$\Psi_{iso} = -\frac{\mu}{2} I_{max} \log \left(1 - \frac{I_1 - 3}{I_{max}} \right)$$

$\Psi_{ani} = c_1(I_4 - 1) - \frac{c_1}{2}(I_5 - 1)$ <p style="text-align: center;">Park and Youn [14]</p>
$\Psi_{ani} = c_1(I_4 - 1) + c_2(I_4 - 1)^2 - \frac{c_1}{2}(I_5 - 1)$ <p style="text-align: center;">Bonet and Burton [15]</p>
$\Psi_{ani} = c_1(I_5 - 1)^2$ <p style="text-align: center;">Merodio and Ogden [16]</p>
$\Psi_{ani} = c_1(2I_4 - I_5 - 1) + c_2(I_5 - 1)^2$ <p style="text-align: center;">Murphy [3]</p>
$\Psi_{ani} = c_1(2I_4 - I_5 - 1) + c_2(I_4 - 1)(I_5 - 1)$ <p style="text-align: center;">Murphy [3]</p>
$\Psi_{ani} = c_1(2I_4 - I_5 - 1) + c_2(I_4 - 1)^2$ <p style="text-align: center;">Murphy [3]</p>
$\Psi_{ani} = c_1(I_5 - I_4^2)$ <p style="text-align: center;">Hollingsworth and Wagner [17]</p>
$\Psi_{ani} = \frac{c_1}{2c_2}(\exp(c_2(I_4 - 1)^2) - 1) + \frac{c_3}{2c_4}(\exp(c_4(I_5 - 1)^2) - 1)$ <p style="text-align: center;">Masson et al. [18]</p>
$\Psi_{ani} = \frac{c_1 + c_2(I_4 - 1)}{c_3 + c_4(I_4 - 1) + c_5(I_4 - 1)^2 + c_6(I_5 - 2I_4 + 1)}$ <p style="text-align: center;">Horgan and Saccomandi [19]</p>

Most of these energies don't have enough degrees of freedom to respect the conditions obtained above, so we will use the last two energies by Horgan and Saccomandi [19] and Masson et. al. [18] as anisotropic parts of our mixture active strain model. The first anisotropic energy that we will use in the mixture active strain approach is the one used by Horgan and Saccomandi in [19].

Considering that in our case:

$$I_4 = \left(\frac{\lambda}{1-\gamma} \right)^2$$

$$I_5 = \left(\frac{\lambda}{1-\gamma} \right)^4$$

the anisotropic stress obtained along \mathbf{m} is the following

$$P_{\mathbf{M}}^{ani} = 2 \frac{\lambda}{(1-\gamma)^2} \frac{c_2}{c_3 + c_4(I_4 - 1) + c_5(I_4 - 1)^2 + c_6(I_5 - 2I_4 + 1)}$$

$$- 2 \frac{\lambda}{(1-\gamma)^2} \frac{(c_1 + c_2(I_4 - 1))(c_4 + 2c_5(I_4 - 1) - 2c_6)}{(c_3 + c_4(I_4 - 1) + c_5(I_4 - 1)^2 + c_6(I_5 - 2I_4 + 1))^2}$$

$$- 4 \frac{\lambda^3}{(1-\gamma)^4} \frac{c_6(c_1 + c_2(I_4 - 1))}{(c_3 + c_4(I_4 - 1) + c_5(I_4 - 1)^2 + c_6(I_5 - 2I_4 + 1))^2}$$

This energy has a quite complex form, and the stress obtained is quite complicated as well. As we can see in Fig. (4.4) the fit on the total curve is quite good. However to reach this result some constants need to be negative, which makes the passive branch of the curve physically unacceptable: in fact this branch doesn't touch the point (1,0), which means that without any activation and any elongation the body can exert a force.

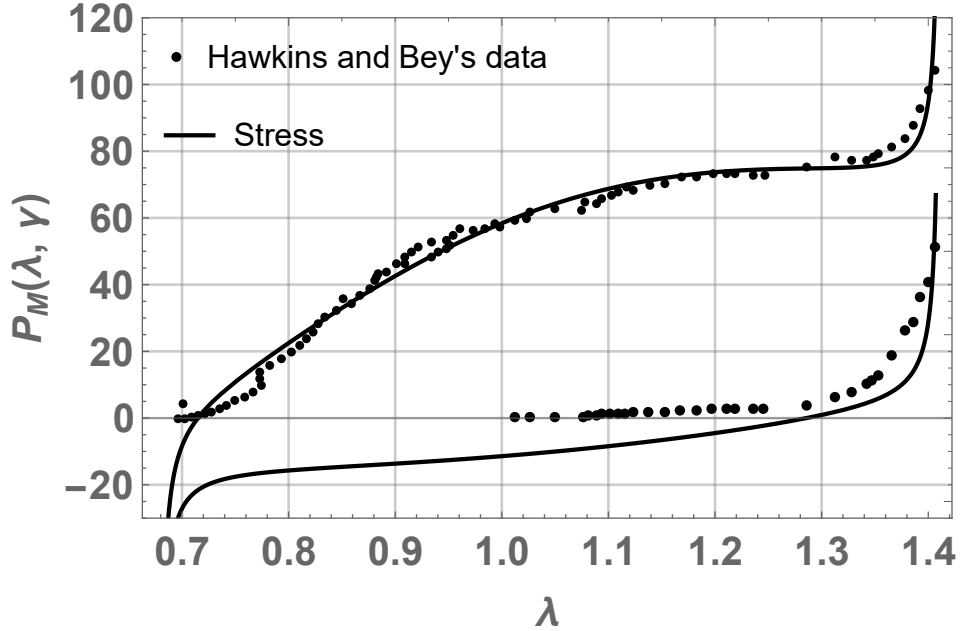


Figure 4.4: Stress-strain relation with energy by Horgan and Saccomandi when $\mu = 1.5$ kPa, $I_{max} = 0.41$, $c_1 = -63.51$ kPa, $c_2 = -10.54$ kPa, $c_3 = 0.62$ kPa, $c_4 = -0.068$ kPa, $c_5 = -0.867$ kPa, $c_6 = -847$ kPa and $\gamma = 0.494$.

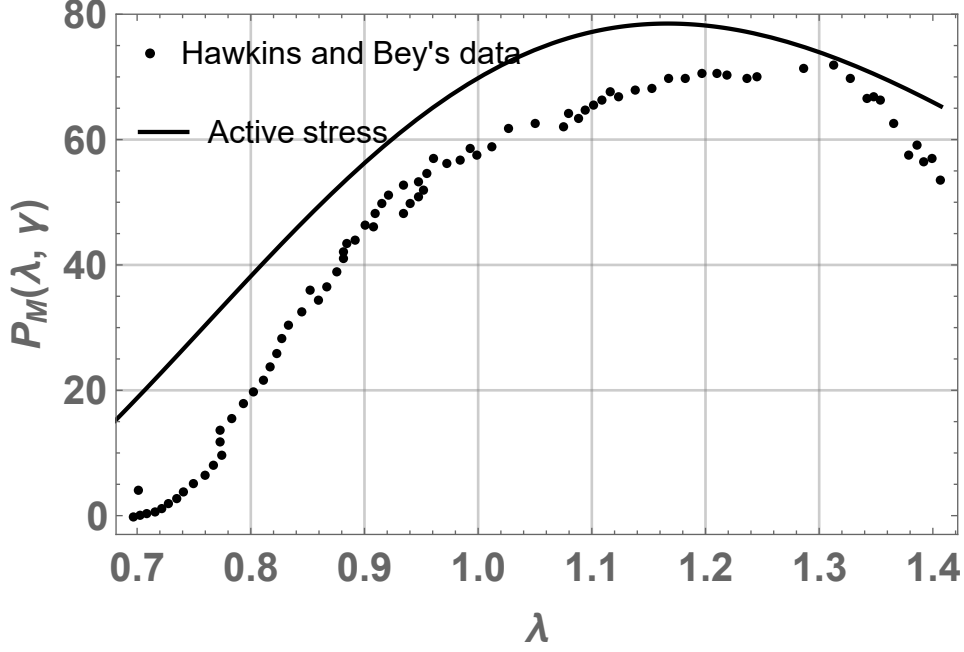


Figure 4.5: Stress-strain relation with active component of the energy by Horgan and Saccomandi when $\mu = 1.5$ kPa, $I_{max} = 0.41$, $c_1 = -63.51$ kPa, $c_2 = -10.54$ kPa, $c_3 = 0.62$ kPa, $c_4 = -0.068$ kPa, $c_5 = -0.867$ kPa, $c_6 = -847$ kPa and $\gamma = 0.494$.

The anisotropic energy used by Masson et. al. [18] has been used for finite dynamic deformations of a hyperelastic, anisotropic, incompressible and prestressed tube.

It's made by two exponential components, each one dependent on only one of the two invariants. The anisotropic part of the component of the first Piola-Kirchhoff stress tensor in the preferential direction \mathbf{m} , is given by

$$P_{\mathbf{M}}^{ani}(\lambda, \gamma) = 2c_1 \left(\exp \left\{ c_2 \left(\left(\frac{\lambda}{1-\gamma} \right)^2 - 1 \right)^2 \right\} - 1 \right) \left(\left(\frac{\lambda}{1-\gamma} \right)^2 - 1 \right) \frac{\lambda}{(1-\gamma)^2} +$$

$$2c_3 \left(\exp \left\{ c_4 \left(\left(\frac{\lambda}{1-\gamma} \right)^4 - 1 \right)^2 \right\} - 1 \right) \left(\left(\frac{\lambda}{1-\gamma} \right)^4 - 1 \right) \frac{\lambda^3}{(1-\gamma)^4}.$$

The results of the following model are plotted in Fig. 4.5, where we set $\mu = 1.5$ kPa, $I_{max} = 0.41$, $c_1 = -1.056$ kPa, $c_2 = 0.201$ kPa, $c_3 = 0.00454$ kPa, $c_4 = -0.0527$ kPa and $\gamma = 0.6$.

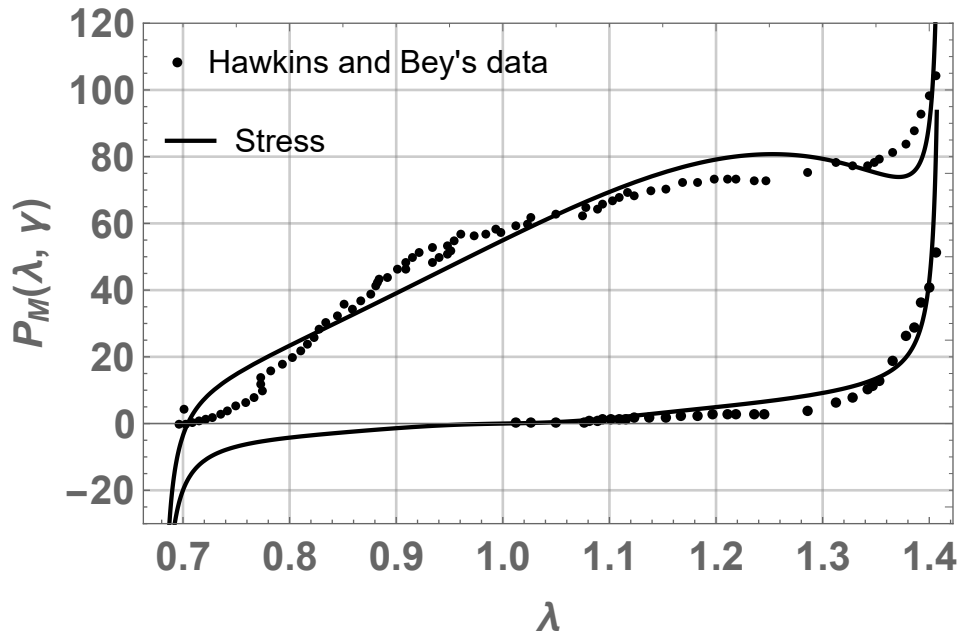


Figure 4.6: Stress-strain relation with energy by Masson et al. when $\mu = 2$ kPa, $I_{max} = 0.41$, $c_1 = -3.501$ kPa, $c_2 = -22.5908$ kPa, $c_3 = 0.044$ kPa, $c_4 = -0.624$ kPa and $\gamma = 0.481$.

The total branch of the curve follows the behaviour of the data quite well, however almost every part of the curve has a quite big error with respect to the data. The passive branch has a really good behaviour, and as it's shown in Fig. 4.6 the active component of the data also follows the experimental data behaviour quite well.

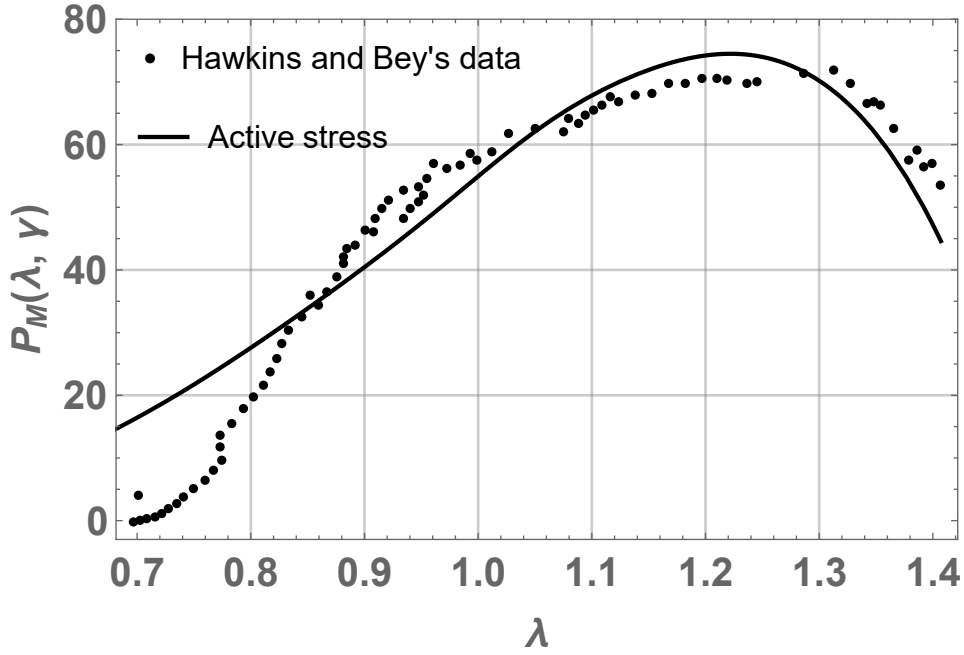


Figure 4.7: Active component of the stress-strain relation with energy by Masson et al. when $\mu = 2$ kPa, $I_{max} = 0.41$, $c_1 = -3.501$ kPa, $c_2 = -22.5908$ kPa, $c_3 = 0.044$ kPa, $c_4 = -0.624$ kPa and $\gamma = 0.481$

Since both these models have a non-linear and complicate dependence on the two invariants, while not fitting the data very well, I decided to use a linear combination of the 3 energies proposed by Murphy.

Originally, in the work by Murphy [3], these energies had an isotropic component made by a Neo-Hookean energy:

$$\Psi_{iso} = c_1(I_1 - 3)$$

but since the Gent energy is a generalization of a Neo-Hookean energy I decided to take only the anisotropic part of these energies into account.

The resulting energy will be:

$$\Psi = -\frac{\mu}{2} I_{max} \log \left(1 - \frac{I_1 - 3}{I_{max}} \right) + c_1(2I_4 - I_5 - 1) + c_2(I_4 - 1)^2 + c_3(I_4 - 1)(I_5 - 1) + c_4(I_5 - 1)^2$$

which gives the following stress along the fibers:

$$\begin{aligned}
P_M(\lambda, \gamma) = & \mu \left(1 - \frac{\lambda^2 + 2\lambda^{-1} - 3}{I_{max}} \right)^{-1} (\lambda - \lambda^{-1}) \\
& + 4c_1 \left(\frac{\lambda}{(1-\gamma)^2} - \frac{\lambda^3}{(1-\gamma)^4} \right) + 2c_2 \left(\frac{\lambda}{(1-\gamma)^2} - 1 \right) \left(\frac{\lambda}{(1-\gamma)^2} \right) \\
& + c_3 \left(\frac{\lambda}{(1-\gamma)^4} - 1 \right) \left(\frac{\lambda}{(1-\gamma)^2} \right) + c_3 \left(\frac{\lambda}{(1-\gamma)^2} - 1 \right) \left(\frac{\lambda^3}{(1-\gamma)^4} \right) \\
& + 2c_4 \left(\frac{\lambda}{(1-\gamma)^4} - 1 \right) \left(\frac{\lambda^3}{(1-\gamma)^4} \right)
\end{aligned}$$

from which we get the following fit:

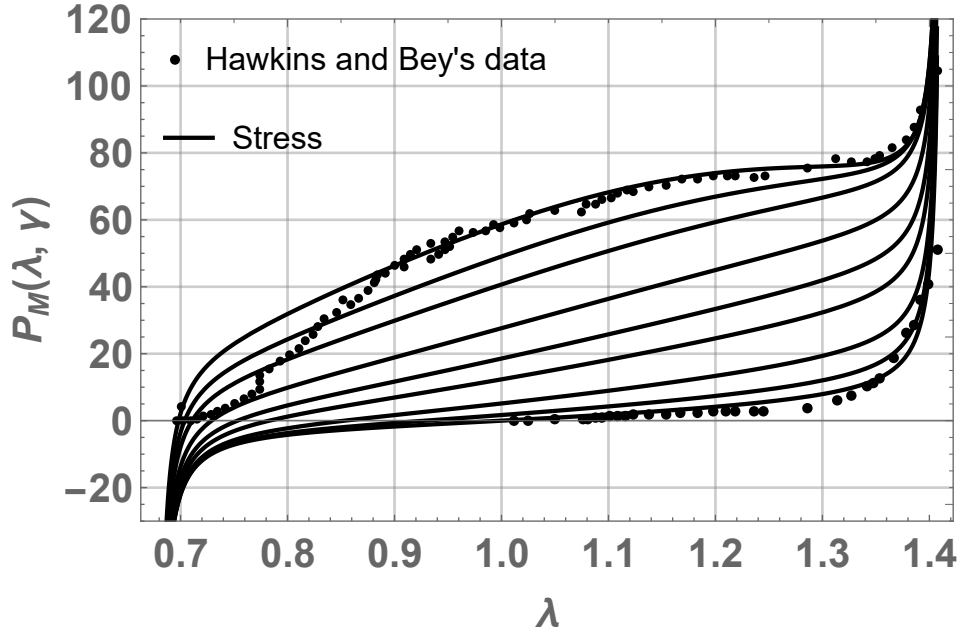


Figure 4.8: Plot of P_M when $\mu = 2.3$ kPa, $I_{max} = 0.41$, $c_1 = 6.21$ kPa, $c_2 = 15.5462$ kPa, $c_3 = -0.3697$ kPa, $c_4 = 0.0116$ kPa and $\gamma = 0.5556$

As we can see in Fig 5.1 the passive branch has a good fit, while for the total fit we can observe that the fit is good for $\lambda > 0.88$, but fails for the other values. In particular we can notice this looking at the active branch in Fig 5.2

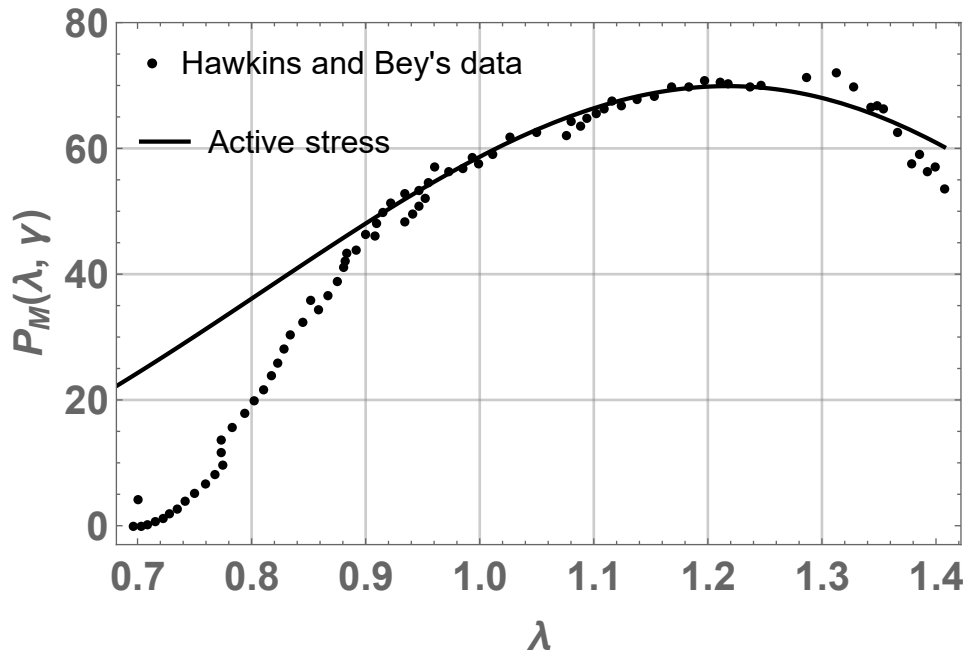
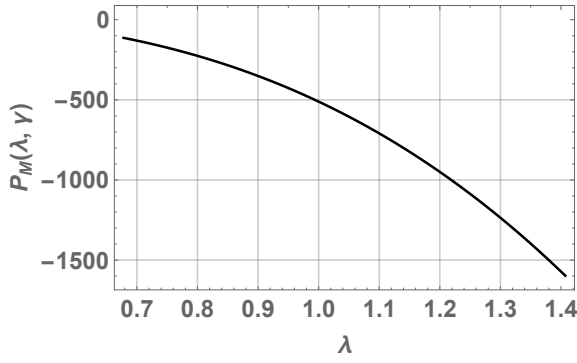
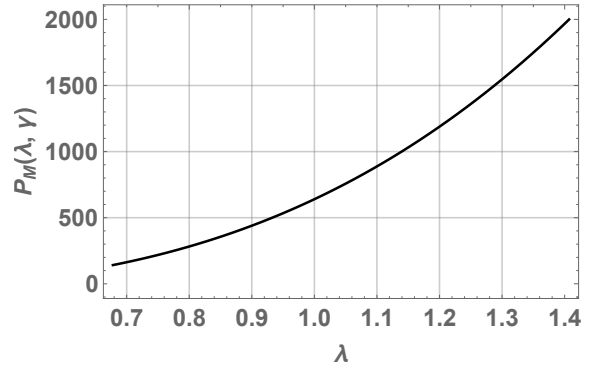


Figure 4.9: Plot of the active part P_M

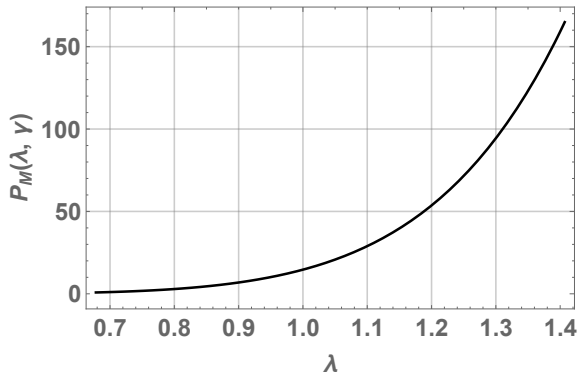
Moreover we can see the contribution to P_M of each activated anisotropic component of the energy:



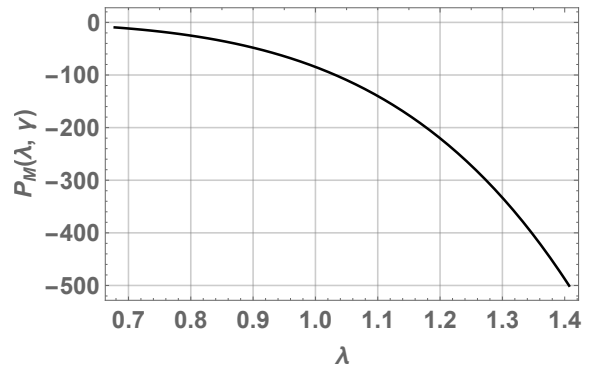
(a) Linear term: $(2I_4 - I_5 - 1)$



(b) Quadratic term : $(I_4 - 1)^2$



(c) Quadratic term : $(I_5 - 1)^2$



(d) Quadratic mixed term : $(I_4 - 1)(I_5 - 1)$

Table 4.1: Contributions of single anisotropic activated terms.

All these energies predict better the data by Hawkins and Bey [4] even with a constant activation using the mixture active strain approach, however polyconvexity of the total energy may not be obtained, or however is not trivial to demonstrate, since I_5 is not polyconvex itself, but its combination with I_4 may be.

Conclusions

In this work we have considered various approaches in order to model muscle tissue. First we introduced two passive energies which reproduce quite well the behaviour of the uniaxial stretch if compared to the experimental results by Hawkins and Bey [4]. Then we introduced two methods to model the active behaviour of muscle tissue, the active stress and the active strain, which have several limitations regarding the mathematical properties of the method, or the possibility to reproduce well the data behaviour. Another method to model active muscle behaviour is the mixture active strain approach, which takes advantage of the Kröner-Lee decomposition only on the anisotropic part of the energy. This method gives the possibility to better reproduce the data even using a constant activation \mathbf{F}_a , which permits to the total energy to inherit the properties of the isotropic part and the anisotropic part of the energy. Finally by introducing the work by Murphy [3] we decided to introduce a new anisotropic energy which depends on both anisotropic invariants I_4 and I_5 , which can reproduce the Hawkins and Bey data almost completely using a constant activation.

Further improvements can be

- Find an energy which better reproduces the lower fit of the energy;
- Find an energy which has a combination of I_5 which is polyconvex, since I_5 itself isn't.

Acknowledgements

The acknowledgements written here aren't just about the degree itself, they're about the journey that this degree has been a part of.

First of all I want to thank the person that made all of this possible, making me the person I am today: my father, the strongest man I know. I want to thank my longtime friends, for always being there at any moment, for supporting me and understanding me even better than myself. Thanks to my family (the blood one and the acquired one), for always being supportive and believing in me. Thanks to my girlfriend, who supported and tolerated me during this last (long) step. Thanks to all the people that I've met thanks to sport and dance, especially the ones that I'm now happy to call friends. Thanks to Alfredo, Giulia and Alessandro for helping and guiding me through the process of writing this work.

Bibliography

- [1] D. Riccobelli, D. Ambrosi, Activation of a muscle as a mapping of stress-strain curves, *Extreme Mechanics Letters*, **28**, 37–42, (2019).
- [2] G. Chagnon, M. Rebouah, D. Favier, Hyperelastic Energy Densities for Soft Biological Tissues: A Review, *Journal of Elasticity*, **120**, 129–160, (2015).
- [3] J. Murphy, Transversely isotropic biological, soft tissue must be modelled using both anisotropic invariants, *Eur. J. Mech. A*, **Solids 42**, 90–96 (2013).
- [4] D. Hawkins and M. Bey. A comprehensive approach for studying muscle-tendon mechanics, *Journal of Biomechanical Engineering*, **116**(1), 51–55, (1994).
- [5] A. N. Gent, A new constitutive relation for rubber, *Rubber Chemistry and Technology*, **69**(1), 59–61, (1996).
- [6] G. Giamtesio, A. Marzocchi, A. Musesti, Loss of mass and performance in skeletal muscle tissue: a continuum model, *Commun. Appl Ind. Math.*, **9**(1), 1–19, (2018).
- [7] A. E. Ehret, M. Böl, M. Itskov, A continuum constitutive model for the active behaviour of skeletal muscle, *Journal of the Mechanics and Physics of Solids*, **59**, no.3, 625–636, (2011).
- [8] G. Giamtesio and A. Musesti, Strain-dependent internal parameters in hyperelastic biological materials, *International Journal of Non-Linear Mechanics*, **95**, 162-167, (2017).
- [9] A. Musesti, Dispense del corso di di Fisica Matematica, a.a. 2019/2020, Università Cattolica del S. Cuore.
- [10] M. Epstein. Mathematical characterization and identification of remodeling, growth, aging and morphogenesis. *Journal of the Mechanics and Physics of Solids*, **84**,72–84, (2015).
- [11] I-S. Liu, *Continuum Mechanics*, Springer, (2002).
- [12] M.E. Gurtin, *An Introduction to Continuum Mechanics*, Academic Press, (1981).
- [13] P. Neff, Some results concerning the mathematical treatment of finite plasticity, *Deformation and Failure in Metallic Materials*, 251–274, (2003).

- [14] H.C. Park, S.K. Youn, Finite element analysis and constitutive modelling of anisotropic nonlinear hyperelastic bodies with convected frames, *Comput. Methods Appl. Mech. Eng.*, **151**, 605–618 (1998).
- [15] J. Bonet, A.J. Burton, A simple orthotropic, transversely isotropic hyperelastic constitutive equation for large strain computations, *Comput. Methods Appl. Mech. Eng.*, **162**, 151–164 (1998).
- [16] J. Merodio, R.W. Ogden, Mechanical response of fiber-reinforced incompressible non-linearly elastic solids, *Int. J. Non-Linear Mech.*, **40**, 213–227 (2005).
- [17] N.T. Hollingsworth, D.R. Wagner, Modeling shear behavior of the annulus fibrosus, *J. Mech. Behav. Biomed. Mater.*, **4**, 1103–1114 (2011).
- [18] I. Masson, C. Fassot, M. Zidi, Finite dynamic deformations of a hyperelastic, anisotropic, incompressible and prestressed tube. Applications to in vivo arteries, *Eur. J. Mech. A, Solids* **29**, 523–529, (2010).
- [19] C.O. Horgan, G. Saccomandi, A new constitutive theory for fiber-reinforced incompressible nonlinearly elastic solids, *J. Mech. Phys. Solids*, **53**, 1985–2015 (2005).
- [20] J. Merodio, R.W. Ogden, Mechanical response of fiber-reinforced incompressible non-linearly elastic solids, *International Journal of Non-Linear Mechanics*, **40**, 213–227. (2005).
- [21] J.A. Weiss, B.N. Maker, S. Govindjee, Finite element implementation of incompressible, transversely isotropic hyperelasticity. *Computer Methods in Applied Mechanics and Engineering*, **135**, 107–128.(1996).
- [22] R. Sinkus, M. Tanter, S. Catheline, J. Lorenzen, C. Kuhl, E. Sondermann, M. Fink, Imaging anisotropic and viscous properties of breast tissue by magnetic resonance-elastography, *Magnetic Resonance in Medicine*, **53**, 372–387,(2005).
- [23] J.-L. Gennisson, S. Catheline, S. Chaffa, M. Fink, Transient elastography in anisotropic medium: application to the measurement of slow and fast shear wave speeds in muscles, *Journal of the Acoustical Society of America*, **114**, 536–541,(2003).
- [24] K.B. Arbogast, S.S. Margulies, Material characterization of the brainstem from oscillatory shear tests, *Journal of Biomechanics*, **31**, 801–807, (1998).
- [25] S.A. Kruse, J.A. Smith, A.J. Lawrence, M.A. Dresner, A. Manduca, J.F. Greenleaf, R.L. Ehman, Tissue characterization using magnetic resonance elastography: preliminary results, *Physics in Medicine and Biology*, **45**, 1579–1590, (2000).
- [26] R.D. Kriz, W.W. Stinchcomb, Elastic moduli of transversely isotropic graphite fibers and their composites, *Experimental Mechanics*, **19**, 41–49, (1979).
- [27] D.A. Morrow, T.L. Haut Donahue, G.M. Odegard, K.R. Kaufman, Transversely isotropic tensile material properties of skeletal muscle tissue, *The Journal of the Mechanical Behavior of Biomedical Materials*, **3**, 124–129. (2010).

- [28] S. Dokos, B.H. Smaill, A.A. Young, I.J. LeGrice, Shear properties of passive ventricular myocardium, *American Journal of Physiology-Heart and Circulatory Physiology*, **283**, H2650–H2659, (2002).